REMARKS

Claims 1-20 and 28 were examined in this case. Of these, claims 3-5, 9-14, and 17 stand rejected under 35 U.S.C. § 112, second paragraph. Claims 1-20 and 28 stand rejected under 35 U.S.C. § 112, first paragraph. And claims 1-10 and 17-20 stand rejected under 35 U.S.C. § 102. In addition, the drawings have been objected to. Each of these issues is addressed below.

Amendments

Claims 1 and 11-16 have been amended, and new claims 29-42 have been added. Support for these amendments is found in the specification, for example, as follows: claim 1, original claims 2 and 3; claims 11-16, original claim 1; new claim 29, original claim 14; new claim 30, page 17, ll. 10-23; new claim 31, original claim 4; new claim 32, original claim 5; new claim 33, original claim 7; new claim 34, original claim 8; new claim 35, original claim 9; new claim 36, original claim 10; new claims 37 and 38, original claim 17; new claim 39, original claim 18; new claim 40, original claim 19; new claim 41, original claim 20; and new claim 42, original claim 27. These amendments add no new matter.

Drawings

The Office has objected to the drawings based on informalities. New drawings are submitted herewith. These drawings differ from the original figures only in the placement and size of the figure legends.

Rejections under 35 U.S.C. § 112, second paragraph

Claims 3-5, 9-14, and 17 stand rejected, under 35 U.S.C. § 112, second paragraph as being indefinite.

In particular, claim 3 stands rejected based on the term "N-terminus." This claim

AMENDMENTS TO THE DRAWINGS

The attached sheets of drawings include changes to Figs. 1-4. These sheets replace the original sheets, Figs. 1-4. In these figures, the figure identifiers have been increased in size and placed below the figures to correct the arrangement of views.

Attachments: Replacement sheets

Annotated Sheet Showing Changes

is now canceled but its language is incorporated into claim 1. The Office states that the N-terminus is not defined as a domain or a specific set of base pairs and is a term that can strictly define the alpha amide end or describe the portion of the protein associated with this amino-terminal end. As is clear from Applicants' specification, it is this latter definition that is utilized in the present specification. The Office is directed, for example, to page 7, where the specification states:

> In another preferred embodiment, the mutation(s) are located at the N terminus of the structural protein, because it has been found that, for example, in the case of the parvoviruses CPV and B19 the N terminus is located on the cell surface. In this case, *the mutation is preferably not carried out directly at the N terminus of VP1 but is carried out a few amino acids downstream from the N terminus.*

Thus, this passage makes clear that it is not the alpha amide end, but rather the region associated with that end of a structural protein that is intended by Applicants' claim language. The indefiniteness rejection based on the term "N terminus" should be withdrawn.

Claim 4 also stands rejected based on the assertion that the term "the protein-cell membrane receptor interaction" lacks antecedent basis. Claim 4 has been canceled but is newly presented as claim 31. The term at issue has been removed from this claim, and the rejection may be withdrawn.

Claim 9 stands rejected based on the assertion that it is unclear how an "insertion" can be "a cell membrane receptor ligand, a Rep protein,..." etc. Claim 9 has been canceled, but is newly presented as claim 35. In this new claim, it is clarified that the insertion into the structural protein is at least one of the listed components. Further, the "and/or" language has been removed. This basis for the rejection may be withdrawn.

Claim 10 also stands rejected because of the use of the term "and/or" and because "integrin" is listed twice in the claim. Claim 10 has been canceled and newly presented as claim 36. In claim 36, the "and/or" language has been removed and integrin is listed

only once. This basis for the rejection may be withdrawn.

Claims 11-13 stand rejected as being indefinite because these claims refer to particular endonuclease cleavage sites without specifying a reference sequence. This rejection is respectfully traversed. Claims 11-13 do indeed provide the reference sequence VP1. This sequence was publicly available as of the filing date of the present specification (see, for example, NCBI Accession No. 2906023 (1998) (Exhibit 3) and Ruffing et al., J. Gen. Virol. 75:3385-3392 (1994) (Exhibit 4)). No further description in Applicants' specification is therefore necessary, and this rejection may be withdrawn.

Claims 13-14 stand further rejected on the basis that the metes and bounds of the term "one or more insertions" is unclear. To clarify this term, the insertions in claim 13 are indicated to be DNA insertions and the insertions in claim 14 to be amino acid insertions. The term "one or more" simply indicates that a single, or multiple, insertions may be made at the indicated site(s). As indicated in Applicants' specification, these insertions may be any sequence that increases the infectivity of AAV. This rejection of claims 13-14 may be withdrawn.

Claim 17 stands rejected as being unclear in its recitation that the structural protein is in the "form of an AAV particle, particularly a capsid" and in the use of the term "a" structural protein. Claim 17 has been canceled and is presented now as claims 37 and 38. These claims have been amended to overcome this rejection. Claim 37 now states that the "structural protein is a component of an AAV particle," and claim 38 states that the "structural protein is a component of the capsid." In addition, the claims now refer to "the" rather than "a" structural protein. This final basis for the indefiniteness rejection may be withdrawn.

Rejection under 35 U.S.C. § 102

Claims 1-10 and 17-20 stand further rejected, under 35 U.S.C. § 102, as being anticipated by Mamounas et al. (WO 97/38723). This rejection is respectfully traversed,

and the rejection as applied to each of Applicants' current independent claims is now addressed.

Taking the claims in turn, Mamounas does not anticipate present claims 1 or 15 or their dependent claims because Mamounas fails to teach a structural protein of AAV that is "capable of particle formation," as required by these claims. As stated by Mamounas, at page 68, lines 13-14, the rAAV chimeric virion tested by the authors "failed to produce any intact viral particles."

In maintaining the present rejection, the Office states that this passage of Mamounas merely teaches that "*initial attempts* to make one of their AAV mutant particles failed. However, upon modification of their transfection system, particles with altered structural proteins were generated (see page 68, line 11 to page 69, line 5)." Applicants do not disagree. However, it is pointed out that it is precisely this necessary modification of the transfection system that evidences the failure of Mamounas to teach the presently claimed invention. In particular, Mamounas states (page 68, ll. 14-18; emphasis added):

> To overcome this obstacle [the failure to produce any intact viral particles], we included *wild type AAV capsid proteins* into the packaging process. We employed a triple plasmid DNA co-transfection strategy, namely co-infecting cells with (1) *pAV/Ad [a rAAV vector encoding wild-type capsid protein; page 64, line 31]*, (2) pAAVgal conjugated to polylysine coupled adenovirus, and (3) the individual pVP-scFv chimeric protein-containing plasmid.

Thus, the only way that Mamounas could produce intact viral particles was to include in their transfection system a helper vector encoding wild-type capsid protein. In Mamounas, it is that wild-type capsid protein that facilitates viral particle formation. In essence, Mamounas makes use of two AAV capsid proteins: one that carries the targeting ligand but does not facilitate particle formation, and a second that facilitates particle formation but does not bring about an increase in AAV infectivity. In contrast, as

described in the present specification, Applicants have developed AAV structural proteins that carry out – in a single structural protein – both functions. Applicants' structural proteins of claims 1 and 15 both increase AAV infectivity *and* facilitate viral particle formation. Mamounas does not describe this type of AAV structural protein and therefore cannot anticipate present claims 1 or 15, or their dependent claims. The rejection of these claims under § 102 should be withdrawn.

Independent claims 11-14 and 16 (and their dependent claims) are also free of the present anticipation rejection because Mamounas fails to describe the particular mutations leading to increased infectivity specified by these claims. On this issue, the Office is directed to Exhibits 1 and 2, the nucleotide and amino acid sequences of AAV structural proteins VP1, VP2, and VP3.

Exhibit 1 shows the DNA sequence of the AAV2 genome according to Ruffing M. et al. 1994, cited in the specification at page 4, ll. 14-16, a sequence that is also available from Medline at:
http://www.ncbi.nlm.nih.gov/entrez/viewer.fcgi?db=nucleotide&val=2906016. In Exhibit 1 the ATG start codon of VP1 (pos. 2203-2205 in the genome sequence), the ACG start codon of the overlapping VP2 (pos. 26143-2616), the ATG start codon of VP3 (pos. 2809-2811), and the common TAA stop codon of the VP1, VP2 and VP3 genes (pos. 4326-4328) have been indicated in bold. In addition, both XhoI sites (C/TCGAG, pos. 2233-2238 and 2419-2424), the BsrBI site (GAG/CGG, pos. 2308-2313), and the HindII site (GTC/AAC, pos. 2395-2400) of the VP1 gene, referred to in independent claims 11-14 and 16, have been underlined.

Exhibit 2 shows the amino acid sequences corresponding to these overlapping VP1, VP2, and VP3 genes. In the amino acid sequence of Exhibit 2, the amino-terminal methionine of VP1 (pos. 1), the amino-terminal threonine of VP2 (pos. 138), and the amino-terminal methonine of VP3 (pos. 203) are indicated in bold. The above-mentioned restriction sites of the VP1 gene, which can be used for mutations according to the

invention, correspond to the positions of leucine 11 (XhoI), glutamic acid 36 / arginine 37 (BsrBI), valine 65 / asparagine 66 (HindII), and leucine 73 (XhoI), respectively, in the VP1 amino acid sequence. In addition, in Exhibit 2, SEQ ID NO: 2 (YKQIS SQSGA, pos. 257-266), SEQ ID NO: 3 (YLTLN NGSQA, pos. 377-386), SEQ ID NO: 4 (YYLSR TNTPS, pos. 443-452), SEQ ID NO: 5 (EEKFF PQSGV, pos. 530-539) SEQ ID NO: 6 (NPVAT EQYGS, pos. 569-578), SEQ ID NO: 7 (LQRGN RQAAT, pos. 583-592), and SEQ ID NO: 8 (NVDFT VDTNG, pos. 709-718), indicated in independent claim 14, have been underlined.

These Exhibits illustrate that Mamounas does not teach the mutations that bring about increased AAV infectivity specified by any of claims 11-14 or 16. Mamounas teaches only one deletion of VP1 asserted to influence viral infectivity, a deletion referred to as "Vp1 hydro," that spans a proline rich region at VP1 amino acids 26-34. This single deleted VP1 protein does not anticipate Applicants' claims. In particular, claim 11 requires that increased infectivity be brought about by a VP1 structural protein having one or more insertions at a XhoI site; these sites occur in VP1 at amino acids 11 and 73. Neither mutation is therefore positioned at the Vp1 hydro site between amino acids 26-34 and so claim 11 is not anticipated by Mamounas. Claim 12 requires that increased infectivity be brought about by a VP1 structural protein having one or more insertions at a BsrBI site, a site that occurs at amino acids 36-37. Again, this position is distinct from the Vp1 hydro deletion of Mamounas, and Mamounas therefore does not anticipate this claim.

Similarly, claims 13 and 16 require that increased AAV infectivity be brought about by particular VP1 deletions. Claim 16 requires that increased infectivity be brought about by one or more deletions between the BsrBI site at amino acids 36/37 and the Hind II site at amino acid positions 65/66, and claim 13 requires that increased infectivity be brought about by one or more of these same deletions in combination with one or more insertions. Again, Mamounas fails to teach these deletions alone or in combination with

insertions, or their ability to increase viral infectivity.

Mamounas also fails to disclose any of the particular VP3 mutations specified in claim 14 as SEQ ID NOS: 2-8. The only VP3 mutation tested by Mamounas, termed D4, spans amino acids 239-244 of Exhibit 2 (see Mamounas p. 4, l. 29-31; p. 61, l. 9-28; p. 62, l. 20-23; p. 62, l. 31-32). This corresponds to amino acids VITTST, a sequence that differs from any of the specified sequences, SEQ ID NOS: 2-8, of claim 14, and furthermore that occurs at a position that is upstream of all of the mutation sites covered by Applicants' claim. These structural proteins of claim 14 (and its dependent claims) are novel over Mamounas, and the rejection of these claims should be withdrawn.

Finally, with respect to independent claims 39-42 (previously, claims 18-20 and 28), Applicants point out that each of these claims requires the limitations of independent claims 1 or 11-16 discussed above. As claims 1 and 11-16 are novel over Mamounas, independent claims 39-42 are novel as well. The § 102 rejections of all claims should be withdrawn.

Rejection under 35 U.S.C. § 112, first paragraph

Finally, claims 1-20 and 28 stand further rejected under 35 U.S.C. § 112, first paragraph based on written description. This rejection turns on the Office's assertion that "there is no clear description of the structural or functional characteristics required for any other mutations [other than I-587] to increase infectivity." As applied to the current claims, this rejection is respectfully traversed.

The current independent claims refer to the following very specific classes of AAV mutations having very specific "structural characteristic" requirements:

(i) claim 1 requires mutations that are surface-located and present in the N-terminus of the structural protein;

(ii) claim 11 requires that the structural protein be VP1 and that it contain an insertion at one or two possible XhoI cleavage sites of the VP1-encoding DNA;

(iii) claim 12 requires that the structural protein be VP1 and that it contain an insertion at the BsrBI cleavage site of the VP1-encoding DNA;

(iv) claim 13 requires that the structural protein be VP1 and that it contain at least one deletion located between the BsrBI and HindII cleavage sites of the VP1-encoding DNA in combination with at least one insertion;

(v) claim 14 requires that the structural protein contain at least one insertion located before and/or after an amino acid of one of seven specified AAV amino acid sequences (SEQ ID NOS: 2-8);

(vi) claim 15 requires that the structural protein be VP1 and that it contain at least one deletion located between the XhoI/XhoI cleavage sites; and

(vii) claim 16 requires that the structural protein be VP1 and that it contain at least one deletion located between the BsrBI/HindII cleavage sites of the VP1-encoding DNA.

In addition, each of these claims requires that the very specific "functional characteristic" that the mutations bring about an increase in AAV infectivity. Thus, each of these claims provides both clear structural and functional limitations, as is required by the written description prong of § 112.

Moreover, Applicants take issue with the Office's position that "it is unclear whether applicants possess the structural proteins recited in claims 1-20 and 28" and that "applicants have not demonstrated that they are in possession of the recited genus of mutated structural proteins that can form particles and have increased infectivity."

First, with respect to independent claims 11-16, there can be no question that Applicants have provided an adequate written description for the *particular* mutations covered by those claims. None of claims 11-16 cover an inappropriately broad genus, as implied by the Office, but rather are directed to specific classes of mutations that occur at specific sites or small regions of the AAV capsid proteins VP1 or VP3. The rejection as applied to these claims should be withdrawn.

In addition, as indicated previously, the assertion that Applicants' specification

fails to provide a written description for a claim such as claim 1 is in error. This claim is also directed to a reasonable number of structural protein species, each of which must have the functional characteristic of being capable of facilitating AAV particle formation and increased AAV infectivity. In addition, claim 1 now has the structural characteristic that the mutation must be positioned in the structural protein's N-terminus. This region has been identified by Applicants as one that is surface-located and therefore both amenable to mutations and available for retargeting the virus to increase its infectivity. As indicated previously by Applicants, this region was not determined by an "empirical" process, but rather was based on sound scientific methodologies set forth in Applicants' specification. In particular, selection of this region as an AAV mutation site was determined by structure and protein alignments of different parvoviruses, such as AAV2, CPV, and B19, as discovered by Applicants and as set forth in the specification at page 5, line 32 et al. and page 6, line 23 et al. At this N-terminal region, insertions may be made that target the virus to particular cell types. Using this same sound scientific reasoning, the specific mutation sites of independent claims 11- 16 were chosen as well.

With respect to insertion sequences, these are readily chosen by one skilled in the art and need not be provided by Applicants. These sequences are tailored to the desired tropism for the virus. Typically, insertion sequences are ligands known to target a cell type of interest. Numerous ligands are available in the art for use for this purpose; a number of preferred insertion sequences are provided by Applicants at page 8, line 4 – page 10, line 22.

Contrary to the Office's assertion, Applicants have demonstrated the effectiveness of their strategy using the P1 ligand as an exemplary targeting insertion. The P1 ligand was selected due to the presence of the RGD motif, a motif responsible for binding to the integrin receptor (see page 9, lines 32-34). This ligand was chosen because of its known cell targeting specificity. In the specification, for example, at Tables 1 and 2, Applicants demonstrate that mutated structural proteins that include the exemplary P1 ligand

insertion (in either VP1 or VP3) support viral particle formation; this is shown unambiguously by the data in the columns denoted "Capsid titers," where ELISAs are performed using the antibody A20Mab, an antibody that only recognizes assembled viral capsids.

Similarly, at page 28, Applicants describe additional VP3 insertions of an unrelated sequence, the Z34C domain of protein A. Applicants have provided evidence (Ried et al., J. Virol. 76:4559-4566, 2002) that this AAV structural protein mutant supports formation of viral particles and facilitates re-targeting of cell infectivity. The Office dismisses this evidence, stating that "increased infectivity of the mutant is not disclosed." Applicants disagree. The Office is directed to page 4559, second column, of Ried which states:

> By use of *Z34C* insertion mutants, *rAAV was retargeted* to hematopoietic cell lines which were poorly transduced by rAAV carrying the wild-type capsid via a specific interaction with the cell surface receptor CD29 (β_1-integrin), CD117 (c-kit), or CXCR4.

Thus, this publication specifically states that the Z34C mutation described by Applicants retargets AAV -- i.e., increases AAV infectivity.

As further evidence, Applicants have provided to the Office references by Grifman et al. (Mol. Therapy 3:964-975, 2001) and Nicklin et al. (Mol. Therapy 4: 174-181, 2001, Abstract), demonstrating that ligands other than P1 can be inserted into AAV structural proteins and result in mutated proteins that support viral particle formation and re-targeting of infectivity. The Office has also dismissed this evidence, stating that these references "describe the generation of particles that have mutated structural proteins. Some of the resultant particles have impaired transduction (see page 970, Grifman) and some have altered tropism, whether or not their infectivity is increased is unknown." Again, Applicants point out that "altered tropism" *is* increased infectivity, as it results in

AAV's ability to infect cells not previously available as hosts. Once more, Applicants request that the Office consider this evidence. With respect to Grifman, Applicants also particularly point out that this reference demonstrates that, just as taught by Applicants, a structural protein having an insertion at SEQ ID NO: 7 (of claim 14) results in altered tropism (see, for example, Figure 6). Again, this supports both the efficacy of the structural protein covered by Applicants' specific claim 14 as well as the underlying methodology by which Applicants have identified AAV structural proteins having increased infectivity.

Further, on this issue, Applicants submit herewith one additional publication for the Office's consideration. This reference, Wu et al. (J. Virol. 74:8635-8647, 2000; Exhibit 5) describes a series of AAV surface mutants. While altered infectivity of these mutants was not tested, the reference describes six mutants that were capable of presenting foreign epitopes or ligands for AAV retargeting to alternative receptors (see page 8645, left column, last paragraph). The mutant "aa 266" corresponds to Applicants' mutant structural protein having insertion site SEQ ID NO: 2, and mutant "aa 591" corresponds to Applicants' mutant structural protein having insertion site SEQ ID NO: 7, again confirming both Applicants' general strategy for producing structural proteins falling within the claims and the specific structural proteins of claim 14.

In view of the above, it is clear that Applicants do describe in their specification an effective, general strategy for producing AAV structural proteins that facilitate increased viral infectivity. It is also clear that Applicants' specification discloses not one, but many, species falling under the present claims, and on this point the Office appears to be in agreement. As amended, Applicants' claims are directed to particular mutant proteins having very defined structural and functional characteristics. For these claims, the written description requirement has been satisfied, and this rejection should be withdrawn.

CONCLUSION

Applicant submits that the claims are now in condition for allowance, and such action is respectfully requested.

Enclosed are a Petition to extend the period for replying to the Office action for three months, to and including November 18, 2004, and a check in payment of the required extension fee.

If there are any additional charges or any credits, please apply them to Deposit Account No. 03-2095.

Respectfully submitted,

Date: 18 November 2004

Karen L. Elbing, Ph.D.
Reg. No. 35,238

Clark & Elbing LLP
101 Federal Street
Boston, MA 02110
Telephone: 617-428-0200
Facsimile: 617-428-7045

EXHIBIT 1

Ruffing,M., Heid,H. and Kleinschmidt,J.A., Mutations in the carboxy terminus of adeno-associated virus 2 capsid proteins affect viral infectivity: lack of an RGD integrin-binding motif, J. Gen. Virol. 75 (Pt 12), 3385-3392 (1994)
HTTP://WWW.NCBI.NLM.NIH.GOV/ENTREZ/VIEWER.FCGI?DB=PROTEIN&VAL=2906023

```
   1 ttggccactc cctctctgcg cgctcgctcg ctcactgagg ccgggcgacc aaaggtcgcc
  61 cgacgcccgg gctttgcccg ggcggcctca gtgagcgagc gagcgcgcag agagggagtg
 121 gccaactcca tcactagggg ttcctggagg ggtggagtcg tgacgtgaat tacgtcatag
 181 ggttagggag gtcctgtatt agaggtcacg tgagtgtttt gcgacatttt gcgacaccat
 241 gtggtcacgc tgggtattta agcccgagtg agcacgcagg gtctccattt tgaagcggga
 301 ggtttgaacg cgcagccgcc atgccggggt tttacgagat tgtgattaag gtccccagcg
 361 accttgacga gcatctgccc ggcatttctg acagctttgt gaactgggtg gccgagaagg
 421 aatgggagtt gccgccagat tctgacatgg atctgaatct gattgagcag gcacccctga
 481 ccgtggccga gaagctgcag cgcgactttc tgacggaatg gcgccgtgtg agtaaggccc
 541 cggaggccct tttctttgtg caatttgaga agggagagag ctacttccac atgcacgtgc
 601 tcgtggaaac caccggggtg aaatccatgg ttttgggacg tttcctgagt cagattcgcg
 661 aaaaactgat tcagagaatt taccgcggga tcgagccgac tttgccaaac tggttcgcgg
 721 tcacaaagac cagaaatggc gccggaggcg ggaacaaggt ggtggatgag tgctacatcc
 781 ccaattactt gctccccaaa acccagcctg agctccagtg ggcgtggact aatatggaac
 841 agtatttaag cgcctgtttg aatctcacgg agcgtaaacg gttggtggcg cagcatctga
 901 cgcacgtgtc gcagacgcag gagcagaaca aagagaatca gaatcccaat tctgatgcgc
 961 cggtgatcag atcaaaaact tcagccaggt acatggagct ggtcgggtgg ctcgtggaca
1021 aggggattac ctcggagaag cagtggatcc aggaggacca ggcctcatac atctccttca
1081 atgcggcctc caactcgcgg tcccaaatca aggctgcctt ggacaatgcg ggaaagatta
1141 tgagcctgac taaaaccgcc cccgactacc tggtgggcca gcagcccgtg gaggacattt
1201 ccagcaatcg gatttataaa attttggaac taaacgggta cgatccccaa tatgcggctt
1261 ccgtctttct gggatgggcc acgaaaaagt tcggcaagag gaacaccatc tggctgtttg
1321 ggcctgcaac taccgggaag accaacatcg cggaggccat agcccacact gtgcccttct
1381 acgggtgcgt aaactggacc aatgagaact ttcccttcaa cgactgtgtc gacaagatgg
1441 tgatctggtg ggaggagggg aagatgaccg ccaaggtcgt ggagtcggcc aaagccattc
1501 tcggaggaag caaggtgcgc gtggaccaga aatgcaagtc ctcggcccag atagacccga
1561 ctcccgtgat cgtcacctcc aacaccaaca tgtgcgccgt gattgacggg aactcaacga
1621 ccttcgaaca ccagcagccg ttgcaagacc ggatgttcaa atttgaactc acccgccgtc
1681 tggatcatga ctttgggaag gtcaccaagc aggaagtcaa agacttttc cggtgggcaa
1741 aggatcacgt ggttgaggtg gagcatgaat tctacgtcaa aaagggtgga gccaagaaaa
1801 gacccgcccc cagtgacgca gatataagtg agcccaaacg ggtgcgcgag tcagttgcgc
1861 agccatcgac gtcagacgcg gaagcttcga tcaactacgc agacaggtac caaaacaaat
1921 gttctcgtca cgtgggcatg aatctgatgc tgtttccctg cagacaatgc gagagaatga
1981 atcagaattc aaatatctgc ttcactcacg gacagaaaga ctgtttagag tgctttcccg
2041 tgtcagaatc tcaacccgtt tctgtcgtca aaaaggcgta tcagaaactg tgctacattc
2101 atcatatcat gggaaaggtg ccagacgctt gcactgcctg cgatctggtc aatgtggatt
2161 tggatgactg catctttgaa caataaatga tttaaatcag gtatggctgc cgatggttat
2221 cttccagatt ggctcgagga cactctctct gaaggaataa gacagtggtg gaagctcaaa
2281 cctggcccac caccaccaaa gcccgcagag cggcataagg acgacagcag gggtcttgtg
2341 cttcctgggt acaagtacct cggacccttc aacggactcg acaagggaga gccggtcaac
2401 gaggcagacg ccgcggccct cgagcacgac aaagcctacg accggcagct cgacagcgga
2461 gacaacccgt acctcaagta caaccacgcc gacgcggagt ttcaggagcg ccttaaagaa
2521 gatacgtctt ttgggggcaa cctcggacga gcagtcttcc aggcgaaaaa gagggttctt
2581 gaacctctgg gcctggttga ggaacctgtt aagacggctc cgggaaaaaa gaggccggta
2641 gagcactctc ctgtggagcc agactcctcc tcgggaaccg gaaaggcggg ccagcagcct
2701 gcaagaaaaa gattgaattt tggtcagact ggagacgcag actcagtacc tgacccccag
2761 cctctcggac agccaccagc agccccctct ggtctgggaa ctaatacgat ggctacaggc
2821 agtggcgcac caatggcaga caataacgag ggcgccgacg gagtgggtaa ttcctcggga
2881 aattggcatt gcgattccac atggatgggc gacagagtca tcaccaccag cacccgaacc
```

EXHIBIT 2

Ruffing,M., Heid,H. and Kleinschmidt,J.A., Mutations in the carboxy terminus of adeno-associated virus 2 capsid proteins affect viral infectivity: lack of an RGD integrin-binding motif, J. Gen. Virol. 75 (Pt 12), 3385-3392 (1994)
HTTP://WWW.NCBI.NLM.NIH.GOV/ENTREZ/VIEWER.FCGI?DB=PROTEIN&VAL=2906023

MAADGYLPDWLEDTLSEGIRQWWKLKPGPPPPKPAERHKDDSRGLVLPGYKYLGPFNGLD 60
KGEPVNEADAAALEHDKAYDRQLDSGDNPYLKYNHADAEFQERLKEDTSFGGNLGRAVFQ 120
AKKRVLEPLGLVEEPVKTAPGKKRPVEHSPVEPDSSSGTGKAGQQPARKRLNFGQTGDAD 180
SVPDPQPLGQPPAAPSGLGTNTMATGSGAPMADNNEGADGVGNSSGNWHCDSTWMGDRVI 240
TTSTRTWALPTYNNHLYKQISSQSGASNDNHYFGYSTPWGYFDFNRFHCHFSPRDWQRLI 300
NNNWGFRPKRLNFKLFNIQVKEVTQNDGTTTIANNLTSTVQVFTDSEYQLPYVLGSAHQG 360
CLPPFPADVFMVPQYGYLTLNNGSQAVGRSSFYCLEYFPSQMLRTGNNFTFSYTFEDVPF 420
HSSYAHSQSLDRLMNPLIDQYLYYLSRTNTPSGTTTQSRLQFSQAGASDIRDQSRNWLPG 480
PCYRQQRVSKTSADNNNSEYSWTGATKYHLNGRDSLVNPGPAMASHKDDEEKFFPQSGVL 540
IFGKQGSEKTNVDIEKVMITDEEEIRTTNPVATEQYGSVSTNLQRGNRQAATADVNTQGV 600
LPGMVWQDRDVYLQGPIWAKIPHTDGHFHPSPLMGGFGLKHPPPQILIKNTPVPANPSTT 660
FSAAKFASFITQYSTGQVSVEIEWELQKENSKRWNPEIQYTSNYNKSVNVDFTVDTNGVY 720
SEPRPIGTRYLTRNL*
LLVNQ*TV*FVSVELWSLRISFLSSFHGYVDK*HGGLIINYKEP
LVMELATPSLRARSLTEAGRPKVARRPGFARAASVSERARREGVA

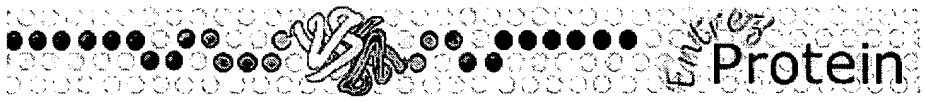


```
LOCUS       AAC03780                735 aa            linear   VRL 24-FEB-1998
DEFINITION  major coat protein VP1 [adeno-associated virus 2].
ACCESSION   AAC03780
VERSION     AAC03780.1  GI:2906023
DBSOURCE    locus AF043303 accession AF043303.1
KEYWORDS    .
SOURCE      Adeno-associated virus 2
  ORGANISM  Adeno-associated virus 2
            Viruses; ssDNA viruses; Parvoviridae; Parvovirinae; Dependovirus.
REFERENCE   1  (residues 1 to 735)
  AUTHORS   Ruffing,M., Heid,H. and Kleinschmidt,J.A.
  TITLE     Mutations in the carboxy terminus of adeno-associated virus 2
            capsid proteins affect viral infectivity: lack of an RGD
            integrin-binding motif
  JOURNAL   J. Gen. Virol. 75 (Pt 12), 3385-3392 (1994)
  MEDLINE   95088582
   PUBMED   7996133
REFERENCE   2  (residues 1 to 735)
  AUTHORS   Berns,K.I., Bohenzky,R.A., Cassinotti,P., Colvin,D., Donahue,B.A.,
            Dull,T., Horer,M., Kleinschmidt,J.A., Ruffing,M., Snyder,R.O.,
            Tratschin,J.-D. and Weitz,M.
  TITLE     Direct Submission
  JOURNAL   Submitted (15-JAN-1998) Cell Genesys Inc., 342 Lakeside Dr., Foster
            City, CA 94404, USA
COMMENT     Method: conceptual translation.
FEATURES             Location/Qualifiers
     source          1..735
                     /organism="Adeno-associated virus 2"
                     /db_xref="taxon:10804"
                     /note="changes relative to the original sequence, GenBank
                     Accession Number J01901, have been detected and verified
                     by several different laboratories"
     Protein         1..735
                     /product="major coat protein VP1"
     CDS             1..735
                     /coded_by="AF043303.1:2203..4410"
ORIGIN
        1 maadgylpdw ledtlsegir qwwklkpgpp ppkpaerhkd dsrglvlpgy kylgpfngld
       61 kgepvneada aalehdkayd rqldsgdnpy lkynhadaef qerlkedtsf ggnlgravfq
      121 akkrvleplg lveepvktap gkkrpvehsp vepdsssgtg kagqqparkr lnfgqtgdad
      181 svpdpqplgq ppaapsglgt ntmatgsgap madnnegadg vgnssgnwhc dstwmgdrvi
      241 ttstrtwalp tynnhlykqi ssqsgasndn hyfgystpwg yfdfnrfhch fsprdwqrli
      301 nnnwgfrpkr lnfklfniqv kevtqndgtt tiannltstv qvftdseyql pyvlgsahqg
      361 clppfpadvf mvpqygyltl nngsqavgrs sfycleyfps qmlrtgnnft fsytfedvpf
      421 hssyahsqsl drlmnplidq ylyylsrtnt psgtttqsrl qfsqagasdi rdqsrnwlpg
      481 pcyrqqrvsk tsadnnnsey swtgatkyhl ngrdslvnpg pamashkdde ekffpqsgvl
      541 ifgkqgsekt nvdiekvmit deeeirttnp vateqygsvs tnlqrgnrqa atadvntqgv
      601 lpgmvwqdrd vylqgpiwak iphtdghfhp splmggfglk hpppqilikn tpvpanpstt
      661 fsaakfasfi tqystgqvsv eiewelqken skrwnpeiqy tsnynksvnv dftvdtngvy
```

```
      721 seprpigtry ltrnl
//
```

Journal of General Virology (1994), 75, 3385–3392. Printed in Great Britain

Mutations in the carboxy terminus of adeno-associated virus 2 capsid proteins affect viral infectivity: lack of an RGD integrin-binding motif

Michael Ruffing,[1]† Hans Heid[2] and Jürgen A. Kleinschmidt[1]*

[1] *Deutsches Krebsforschungszentrum, Forschungsschwerpunkt Angewandte Tumorvirologie and* [2] *Forschungsschwerpunkt Krebsentstehung und Differenzierung, Im Neuenheimer Feld 242, D-69120 Heidelberg, Germany*

Using site-directed mutagenesis, we tested whether a potential integrin-binding site, (composed of the amino acids RGD) which is predicted in the adeno-associated virus 2 (AAV-2) capsid open reading frame (ORF), plays a role in the infectivity of AAV-2. Nucleotide sequencing of wild-type and mutant capsid protein-coding sequences, however, revealed discrepancies with the published sequence data at several positions, including a frameshift in the carboxy terminus which cancels the RGD motif and extends the capsid ORF by 27 amino acis. This sequence was confirmed by protein sequencing of proteolytic fragments of VP3. Thus, the virus mutant (pTAV-p), in which the intention was to exchange D of the putative RGD motif for E, resulted in replacing I^{480} by S in the newly established ORF. A second virus mutant (pTAV-d), in which the intention was to delete the RGD peptide, in fact gave a shift into the ORF of the originally published sequence. The pTAV-p mutant showed a strongly reduced infectivity compared to wild-type AAV-2, whereas pTAV-d was not infectious at all. Neither mutant accumulated viral ssDNA as detected by Hirt extraction. Analysis of virus particle formation and subcellular localization of the capsid proteins revealed a defect of the mutant capsid proteins in capsid assembly. This shows that the newly established C-terminal sequence of the AAV capsid proteins plays an important role in viral assembly.

Introduction

The adeno-associated virus 2 (AAV-2) is a human parvovirus that needs a helper virus for efficient replication (for reviews see Berns, 1990; Berns & Bohensky, 1987; Muzyczka, 1992). The viral genome encodes four non-structural proteins, termed Rep proteins, which are needed for control of gene expression and DNA replication and are encoded by an open reading frame (ORF) on the left side of the genome (Hermonat *et al.*, 1984; Mendelson *et al.*, 1986; Srivastava *et al.*, 1983; Tratschin *et al.*, 1984). The three capsid proteins (VP1, VP2 and VP3) are encoded by another ORF located on the right side of the genome (Becerra *et al.*, 1985, 1988; Cassinotti *et al.*, 1988; Janik *et al.*, 1984; Srivastava *et al.*, 1983). The structural proteins form an icosahedral capsid 20 to 24 nm in diameter with a stoichiometry of 1:1:10 for VP1:VP2:VP3. They are expressed from different translation initiation codons of the same ORF. The observed stoichiometry of 1:1:10 is generated by the relative abundance of an alternatively spliced mRNA, from which VP1 is translated, and a reduced translation initiation frequency of VP2 from an unusual initiation codon (ACG) at position 2615 (Muralidhar *et al.*, 1994). Assembly studies suggest a two-step assembly process: first empty capsids are formed then the ssDNA virus genome is packaged in these to form mature particles (Myers & Carter, 1980). It is assumed that capsid formation is a prerequisite for the accumulation of ssDNA (Myers & Carter, 1981). Mutations in the VP initiation sites have shown that VP2 and VP3 are sufficient and necessary for the accumulation of single-stranded progeny DNA, whereas VP1 seems to be required for production of infectious particles (Smuda & Carter, 1991; Muralidhar *et al.*, 1994). In addition, besides the two large replication proteins (Rep78 and Rep68) at least one of the small Rep proteins (Rep52 or Rep40) is also required for ssDNA accumulation (Chejanovsky & Carter, 1989).

AAV-2 can infect a wide variety of cell types and seems to multiply productively in any mammalian cell line that can be infected by a helper virus (Muzyczka, 1992). The cellular receptor(s) to which AAV binds has not been identified yet. According to the nucleotide sequence published by Srivastava *et al.* (1983) the amino

† Present address: Hoffmann-LaRoche, Pharmaceutical Research, Preclinical Genetechnology 66/709, Grenzacher Straße, CH4002 Basel, Switzerland.

acid sequence of the three capsid proteins should include an RGD peptide within the carboxy-terminal part. This motif has been identified in numerous proteins and is involved in adhesion to cellular receptors classified as members of the integrin receptor family (Hynes, 1992; Ruoslathi & Pierbacher, 1986, 1987). RGD motif-containing proteins include the capsid proteins of foot-and-mouth-disease virus (Fox *et al.*, 1989) and coxsackie-virus A9 (Roivainen *et al.*, 1991). Using site-directed mutagenesis we set out to test whether this motif exerts a similar function in the AAV-2 capsid proteins.

The construction of these mutants was based on the previously published AAV-2 sequence (Srivastava *et al.*, 1983). Analysis of the resultant plasmids showed that the original sequence was incorrect and that the C terminus extended another 27 amino acids due to frameshifting to an ORF that does not contain the RGD motif. Thus, the mutant plasmids coded for mutant proteins different from those originally anticipated. The phenotype of these mutants suggests that the newly established C terminus of the capsid proteins plays an important role in AAV assembly.

Methods

Transfection of HeLa cells and generation of virus stocks. Transfection of HeLa cells was performed according to Chen & Okayama (1987). For preparation of wild-type and mutant virus stocks 2×10^6 cells were transfected with 15 μg pTAV-2 (Heilbronn *et al.*, 1990), pTAV-p or pTAV-d, respectively, infected with adenovirus type 2 (m.o.i. of 5) and collected from the culture medium 4 to 5 days post-infection. After three freeze-thaw cycles, cellular debris was removed by centrifugation and the supernatant was incubated for 1 h at 56 °C to inactivate the adenovirus.

Mutagenesis and construction of virus mutants. The 2·9 kb *Hin*dIII/*Sst*I fragment comprising the complete sequence encoding the capsid proteins was isolated from the plasmid pTAV-2 (Heilbronn *et al.*, 1990) and cloned into the vector M13mp18. The resulting plasmid mp18-2.9HS was used for site-directed mutagenesis (Taylor *et al.*, 1985) using an Amersham kit following the supplier's instructions. Mutagenesis was performed using the oligonucleotide 5'-GGTCAGCGTGGAGA-GCGAGTGGGAGCT-3' (position 4228 to 4254) to replace nucleotide T at position 4242 [sequence position according to Srivastava *et al.* (1983) and Cassinotti *et al.* (1988)] by G for generation of plasmid pTAV-p and using the oligonucleotide 5'-ACGGGACACGGTCAGC-GAGTGGGAGCTGCA-3' (position 4219 to 4257) to delete the nucleotides from position 4233 to 4242 for generation of plasmid pTAV-d. Mutants were identified by DNA sequencing according to the method of Sanger *et al.* (1977). A 0·3 kb fragment resulting from restriction of the mutated plasmids with *Bbs*pMI and *Sna*BI was isolated and cloned into pTAV-2 replacing the wild-type sequence. These plasmids were sequenced and used for the production of virus stocks.

DNA and protein sequence analysis. Nucleotide sequencing of plasmids pTAV-2 (Heilbronn *et al.*, 1990; Laughlin *et al.*, 1983) and pSM620 (Samulski *et al.*, 1982) was performed according to Sanger *et al.* (1977) using synthetic oligonucleotide primers from the VP3 ORF. Protein sequences of peptides were obtained by digestion of baculo-virus-expressed VP3 protein (Ruffing *et al.*, 1992) with endoproteinase lys C. Briefly, 10^7 Sf9 (*Spodoptera frugiperda*) cells were infected with VP3-recombinant baculoviruses and lysed by sonication (five pulses at power position 6 of a Branson sonifier for 10 seconds, with 50 seconds intervals in ice water) 60 to 72 h later in a buffer containing 1 % NP40, 150 mM-NaCl, 20 mM-Tris–HCl (pH 8), 10 mM-DTT and 5 mM-EDTA. After sedimentation by centrifugation (15 min, 12000 *g* at 4 °C) the pellet was resuspended in 8 M-urea, 20 mM-Tris–HCl (pH 7·5) and incubated for 1 h at room temperature. After centrifugation (15 min, 12000 *g* at 20 °C) the supernatant was separated by SDS–PAGE and transferred to an Immobilon-P membrane (Millipore). The position of VP3 was visualized by staining with Ponceau S. The corresponding region was excised and incubated in a buffer containing 200 mM-Tris–HCl (pH 8), 0·2% Tween-20 and 5 mM-DTT for 1 h at room temperature. After washing the membrane pieces in distilled water, the polypeptides were digested with endoproteinase lys C in a buffer containing 5 M-guanidinium-HCl, 200 mM-Tris–HCl (pH 8) and 5 mM-DTT for 24 h at room temperature and then 2 h at 37 °C. Trifluoroacetic acid was added to a final concentration of 10%. The peptides were purified by HPLC (Applied Biosystems, model 130A; column: Brownlee-C4; length, 100 mm; diameter, 2·1 mm) and sequenced by Edmann degradation (Applied Biosystems, protein sequencer 477A).

Analysis of protein expression. For analysis of protein expression by gel electrophoresis and immunoblotting we prepared total lysates of HeLa cells transfected with pTAV-2, pTAV-p, or pTAV-d, respectively, and infected with adenovirus. Cells were harvested 24 h post-infection and lysed by heating at 100 °C for 5 min in 150 μl sample buffer (Laemmli *et al.*, 1970). After sonication, polypeptides were analysed by SDS–PAGE (Thomas & Kornberg, 1975) and immunoblotting (Harlow & Lane, 1988) using an anti-VP rabbit serum (Ruffing *et al.*, 1992; 1:2000) which recognizes all three capsid proteins, mixed (1:5) with a monoclonal antibody (A69) which recognizes VP1 and VP2 only, to increase the sensitivity for VP1 and VP2 detection. Capsid proteins were visualized by peroxidase-conjugated secondary antibodies and enhanced chemiluminescence detection (Amersham).

For the detection of capsid formation, freeze-thaw lysates of 2×10^6 HeLa cells transfected with pTAV-2, pTAV-p or pTAV-d, respectively, and infected with adenovirus, were sedimented by high-speed centrifugation (3 h, 200000 *g* at 4 °C; Sorvall TH641 rotor). The sediments were analysed by gel electrophoresis and Western blotting.

Analysis of DNA replication. Hirt extracts of HeLa cells transfected with pTAV-2, pTAV-p, or pTAV-d, respectively, and infected by adenovirus-2 were prepared according to Redemann *et al.* (1989) and analysed by Southern blotting using an *Ava*I fragment of 1970 bp comprising the *rep* ORF.

Immunofluorescence analysis. For immunofluorescence, cells were grown on coverslips and transfected as described above. Immuno-fluorescence staining was performed essentially as described by Ruffing *et al.* (1992). In addition to the anti-VP3 serum we used the monoclonal antibody A69 which recognizes VP1 and VP2 only. For double immunofluorescence, undiluted hybridoma supernatants of A69 were mixed with an equal volume of anti-VP3 serum (diluted 1:50 in PBS). Bound antibodies from the VP3 serum were visualized by rhodamine-conjugated secondary antibodies and bound A69 antibodies by fluorescein isothiocyanate-conjugated secondary antibodies.

Results

Generation of viral mutants with alterations of the putative RGD integrin-binding motif and correction of the AAV capsid protein sequence

Changing the amino acid D of the RGD motif into E has been reported to significantly reduce binding of peptides to the integrin receptors of a variety of cells, (Ruoslahti

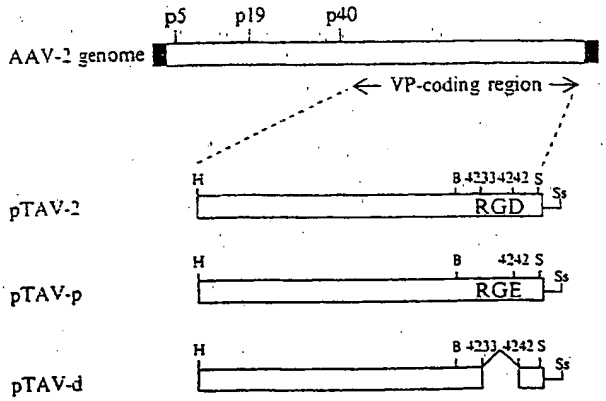

Fig. 1. Intended mutagenesis of the putative RGD peptide in the carboxy-terminal part of the AAV capsid proteins. The AAV-2 genome is depicted, with the inverted terminal repeats indicated by filled rectangular boxes, the three promoters (p) at map unit positions 5, 19 and 40, and the region coding for the capsid proteins (VP) indicated by arrows. Below, the putative RGD peptide of the wild-type genome present in plasmid pTAV-2 and the intended changes in pTAV-p and pTAV-d mutants are shown. The single letters indicate restriction sites used for the generation of the VP mutants: H, *Hin*dIII; B, *Bbs*pMI; S, *Sna*bI and Ss, *Sst*I. The numbers indicate nucleotide positions, according to Srivastava *et al.* (1983) and Cassinotti *et al.* (1988).

& Piersbacher, 1986, 1987). To create this amino acid exchange in the AAV VP-coding sequence, nucleotide 4242 [according to Srivastava *et al.* (1983) and corrected by Cassinotti *et al.* (1988)] was changed from T to G by oligonucleotide-directed mutagenesis. The resultant mutated AAV plasmid was designated pTAV-p ('p' for point mutated). The same method was used to generate the plasmid pTAV-d ('d' for deleted) which lacks the sequence from nucleotide 4233 to 4242 which is supposed to code for the RGD peptide (Fig. 1). Nucleotide sequencing of the VP-coding region of the mutant plasmids and the two wild-type plasmids pTAV-2 (Heilbronn *et al.*, 1990; Laughlin *et al.*, 1983) and pSM620 (Samulski *et al.*, 1982) showed that the published data have to be corrected at several positions (see Table 1). In the amino-terminal part of the shortest capsid protein, VP3, the following corrections have to be made in the coding strand: replace nucleotide C at position 2877 by G; insert the sequence GGCCCG after nucleotide position 3759; replace A at position 3853 by G; insert A after nucleotide position 3891 and delete A at position 3895 [nucleotide positions are given according to Srivastava *et al.* (1983), and corrected by Cassinotti *et al.* (1988)].

Correction of the nucleotide sequence in the carboxy-terminal part includes the deletion of the nucleotide C at position 4227, deletion of C at position 4325, insertion of T after nucleotide 4333 and changes of C (4336) into T and T (4342) into C. The deletion of C at position 4227 results in a frameshift three amino acids upstream of the putative RGD sequence, thus cancelling the RGD motif and extending the capsid protein ORF by 27 amino acids (Fig. 2*a*, reading frame is underlined). The complete amino acid sequence deduced from the corrected nucleotide sequence is shown in Fig. 2(*b*). Amino acid changes are shown in bold letters and are labelled with a dot. The predicted change in the ORF was confirmed by sequencing of peptides obtained by digestion of VP3 expressed in insect cells (Fig. 2*b*, underlined sequences). The baculovirus expression clone of VP3 was derived from pTAV-2 (Heilbronn *et al.*, 1990).

The oligonucleotide used for generation of the pTAV-d mutant was based on the published sequence and overlapped with the sequence corrected at position 4227. Thus it gave rise not only to the deletion of the putative RGD motif, but also to a shift to the ORF of the

Table 1. *Sequence corrections to the AAV-2 VP3 ORF*

Nucleotide position*	Amino acids of the VP3 ORF	Sequence obtained from
Change C(2877) to G	No change	pSM620†, pTAV-2‡
Insert GGC CCG after G(3759)	Insert G and P	pSM620, pTAV-2
Change A(3853) to G	Change N to D	pSM620, pTAV-2, VP3§
Insert A after C(3891)	Change G to R	pSM620, pTAV-2, VP3
Delete A(3895)	No change	pSM620, pTAV-2, VP3
Delete C(4227)	(i) Change H to Q (ii) Frameshift	pSM620, pTAV-2, VP3
Delete C(4325)	Frameshift	pSM620, pTAV-2, VP3
Insert T after T(4333)	(i) Change L to F (ii) Frameshift	pSM620, pTAV-2, VP3
Change C(4336) to T	No change	pSM620, pTAV-2, VP3
Change T(4342) to C	No change	pSM620, pTAV-2, VP3

* Nucleotide positions are given according to Srivastava *et al.* (1983) and corrected by Cassinotti *et al.* (1988).

† Samulski *et al.* (1982).

‡ Heilbronn *et al.* (1990).

§ VP3 amino acid sequences were obtained from VP3 expressed in insect cells according to Ruffing *et al.* (1992).

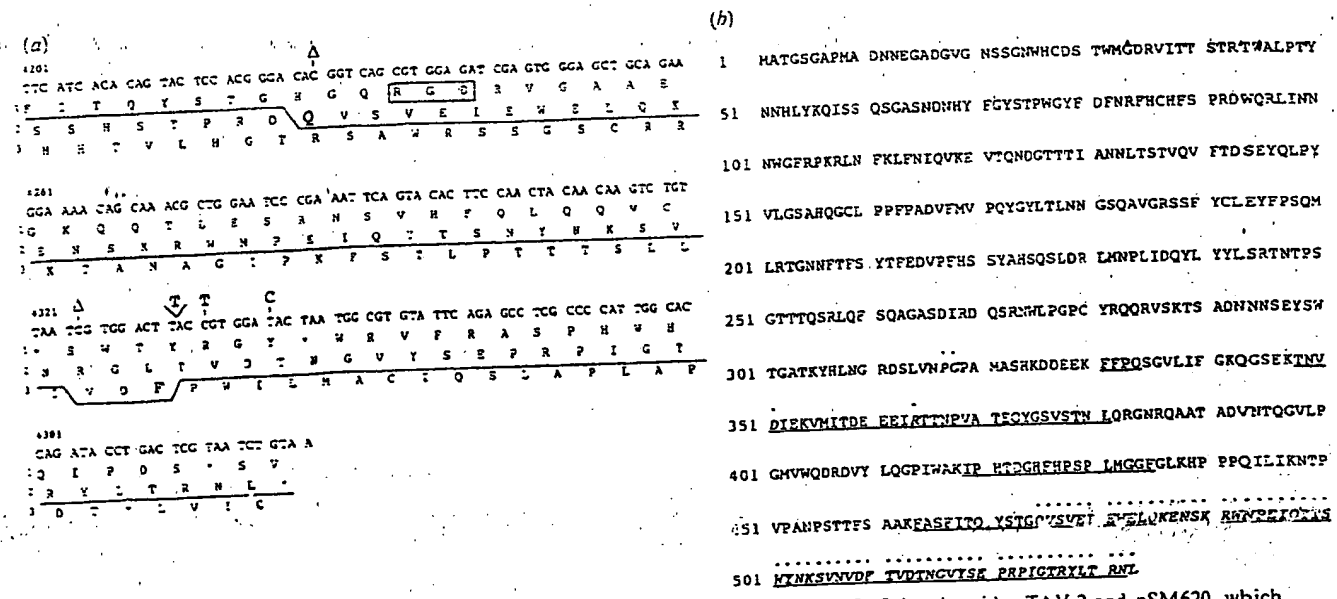

Fig. 2. Corrected amino acid sequence of the AAV-2 capsid proteins. The VP3 ORF of the plasmids pTAV-2 and pSM620, which contain the complete AAV-2 genome cloned from different isolates, were sequenced completely using synthetic primers. Major changes in the reading frame of the C terminus of the capsid proteins are shown at the nucleotide (*a*) and the amino acid (*b*) level. The numbering of the nucleotide sequence is given according to Srivastava *et al.* (1983) and corrected by Cassinotti *et al.* (1988). New sequence corrections are indicated by Δ (for deletion), by ∨ (for insertion) and exchanges are indicated. The three possible ORFs are shown translated under the nucleotide sequence (frames 1, 2 and 3). The ORF according to Srivastava *et al.* (1983) is reading frame 1 containing the RGD sequence motif (rectangle). The predicted ORF based on the corrected nucleotide sequence is underlined. Changed amino acids are marked by bold letters and stop codons by asterisks. (*b*) The complete amino acid sequence of VP3 predicted from the corrected nucleotide sequence, the changes being marked by bold letters and dots. The underlined sequences were confirmed by protein sequencing of peptides, generated from baculovirus-expressed VP3 by digestion with endoproteinase lys C.

published nucleotide sequence. This mutation resulted in the truncation of the capsid proteins by 30 amino acids, which should result in a significantly reduced M_r as observed by gel electrophoresis (see Fig. 4*b*).

The mutant pTAV-p was generated by an oligonucleotide which did not overlap the sequence corrected at position 4227. However, instead of changing the D of the putative RGD tripeptide to E, I^{480} was replaced by S. Taken together, these results show that the AAV-2 capsid proteins in fact do not contain an RGD peptide sequence and that the observed phenotypes of mutant pTAV-p and pTAV-d are based on genetic alterations that are different from those we intended to introduce by site-directed mutagenesis.

Characterization of infectivity of viral mutants pTAV-p and pTAV-d

In order to compare the infectivity of the viral mutants AAV-p and AAV-d with that of wild-type virus, we prepared wild-type and mutant virus stocks by transfection of HeLa cells with the plasmids pTAV-2, pTAV-p, or pTAV-d, respectively, superinfection with adenovirus-2 and lysis of the cells by freezing and thawing. We then infected HeLa cells in parallel with the respective freeze-thaw supernatants after diluting them to equivalent viral DNA contents (Fig. 3*a*) and coinfected with adenovirus. Five days after infection cell-free supernatants were prepared and analysed by dot blot hybridization (Fig. 3*b*).

Limiting dilution of the supernatants showed that the infectivity of AAV-p was reduced about 100-fold compared with that of AAV-2. In the supernatant of pTAV-d-transfected cells no infectivity was detectable. This result was consistent with the assumption that the VP C terminus is important for production of infectious virus.

Expression of the structural and non-structural proteins

To confirm that the AAV non-structural and capsid proteins were expressed in cells transfected by pTAV-p and pTAV-d, respectively, we prepared total cell lysates after superinfection with adenovirus-2 and analysed them by SDS–PAGE and immunoblotting (Fig. 4). The four Rep proteins Rep78, Rep68, Rep52 and Rep40 were detected in equal amounts in cells transfected with

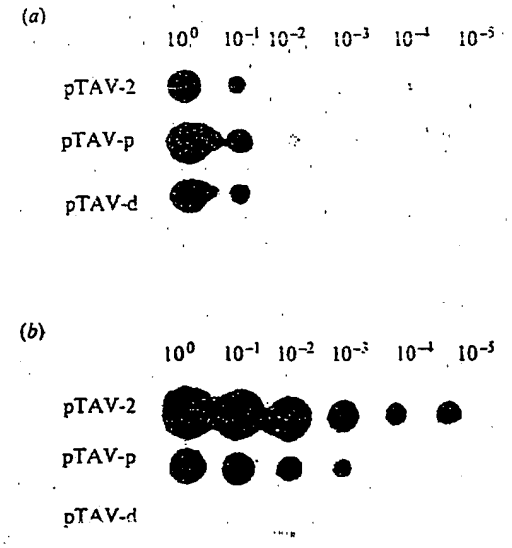

Fig. 3. Reduced infectivity of the mutants AAV-p and AAV-d compared with the wild-type virus AAV-2. (*a*) Cells were transfected with pTAV-2, pTAV-p or pTAV-d, respectively, infected with adenovirus and the culture medium was harvested 4 to 5 days post-infection. For subsequent infection experiments the supernatants containing the putative mutant and wild-type virus stocks were appropriately diluted to obtain equivalent amounts of viral DNA as verified by dot blot hybridization. (*b*) HeLa cells were infected with different dilutions of the supernatants shown in (*a*) and coinfected with adenovirus-2. Cell-free lysates were prepared and analysed in a dot-blot assay by hybridization to a radiolabelled *NdeI–XbaI* fragment of M13mp18–VP3ex (Ruffing *et al.*, 1992).

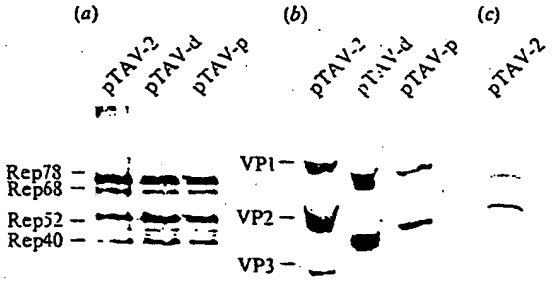

Fig. 4. Expression of Rep and VP proteins in cells transfected with wild-type and mutant plasmids. Total lysates of HeLa cells transfected with pTAV-2, pTAV-d or pTAV-p, respectively, and infected with helper virus, were analysed by gel electrophoresis and immunoblotting. AAV-2 Rep proteins were detected by the monoclonal antibody 303-9 (*a*) and the capsid proteins by a mixture of a polyclonal rabbit antiserum and a monoclonal antibody recognizing VP1 and VP2 (*b*). The specificity of the monoclonal antibody A69 for VP1 and VP2 is shown in (*c*). Rep and VP proteins were visualized by alkaline phosphatase-conjugated secondary antibodies. Aliquots corresponding to 10^4 cells were used. The correct M_r of expressed Rep and VP proteins was checked by coelectrophoresis of an extract of HeLa cells infected with AAV-2 and adenovirus-2 (not shown).

pTAV-p, pTAV-d, or the control plasmid pTAV-2 (Fig. 4*a*). Analysis of capsid protein expression also showed that all of the three capsid proteins VP1, VP2, and VP3 were expressed in cells transfected with the mutant or the control AAV plasmids, respectively (Fig. 4*b*). The greater band intensity of VP1 and VP2 compared with VP3 is due to the enhancement of VP1 and VP2 immunodetection by a VP1/VP2-specific monoclonal antibody (Fig. 4*c*) which was used together with a polyclonal VP antiserum. Structural proteins extracted from cells transfected with pTAV-p comigrated with the wild-type capsid proteins, but those synthesized by the deletion mutant (pTAV-d) had a significantly reduced M_r corresponding with the deletion of the 30 amino acids predicted by the corrected VP sequence (Fig. 4*b*). Taken together, these results mean that the observed phenotypes of the two viral mutants were not due to altered AAV protein expression.

Analysis of ssDNA accumulation and capsid formation

In order to clarify the cause for the reduced infectivity of both viral mutants, we analysed the accumulation of viral ssDNA in HeLa cells after transfection with wild-type and mutant pTAV plasmids and infection with adenovirus-2. In Hirt extracts of cells transfected with pTAV-p or pTAV-d, respectively, no accumulation of AAV ssDNA of defined size could be detected, in contrast to cells transfected with pTAV-2, even after prolonged exposure (Fig. 5*a*). Replicative forms 1 (RF1) and 2 (RF2) of the viral genome were present in all extracts. This means that the replication of the viral genome is obviously not affected by the mutations. Since infectious lysates could be prepared from cells transfected with pTAV-p (Fig. 3*b*), we assumed that in this mutant the efficiency of ssDNA synthesis and/or accumulation is reduced to levels that are undetectable in Hirt extracts. The comparable DNA content of pTAV-p and pTAV-d in freeze-thaw supernatants after transfection and infection with helper virus (Fig. 3*a*) could be due to the transfection input DNA or some release of RF1 and/or RF2 DNA during the freeze-thaw procedure or the cell lysis caused by adenovirus infection.

Since our results did not distinguish whether the low level of ssDNA in Hirt extracts was due to reduced ssDNA synthesis or to less efficient packaging, we analysed the formation of capsid particles which is a prerequisite for DNA packaging (Myers & Carter, 1981). Freeze-thaw lysates of HeLa cells transfected with wild-type or mutated AAV genomes and infected with adenovirus were sedimented by high-speed centrifugation (200000 *g* for 3 h at 4 °C in a Sorvall TH641 rotor) and the sediments were analysed by Western blotting (Fig. 5*b*). Sedimentable capsid proteins were

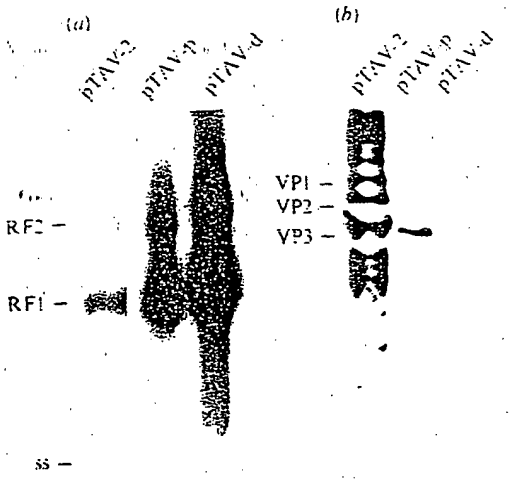

Fig. 5. Analysis of viral ssDNA accumulation and capsid formation. (*a*) Hirt extracts of HeLa cells transfected with pTAV-2, pTAV-p or pTAV-d, respectively, and infected with adenovirus-2 were prepared and analysed by Southern hybridization. Position of the viral ssDNA(ss), the monomeric ds form (RF1) and the dimeric ds form (RF2) are indicated. (*b*) Capsid formation was analysed by high-speed centrifugation of freeze-thaw lysates of HeLa cells transfected with wild-type or mutant plasmids followed by adenovirus infection. Particle formation was detected by gel electrophoresis and Western blotting of the corresponding sediments.

detected in lysates of pTAV-2 transfected cells, whereas there was only a minimal amount of sedimented VP3 from lysates of cells transfected with pTAV-p. We failed to detect sedimentable capsid proteins in lysates of cells transfected with pTAV-d, the mutant which was not infectious at all. This result suggests that the mutants pTAV-p and pTAV-d are defective in viral capsid assembly.

Subcellular distribution of the capsid proteins

Transfection of HeLa cells with pTAV-2, pTAV-p, or pTAV-d, respectively, and infection with adenovirus resulted in different subcellular distribution patterns of the capsid proteins as analysed by indirect immunofluorescence. In most cells transfected with pTAV-2 the AAV capsid proteins were equally distributed in nuclei and cytoplasm when probed with a polyclonal antiserum recognizing all three capsid proteins (Fig. 6*a*). Double immunofluorescence with a monoclonal antibody specific for VP1 and VP2 (see Fig. 4) shows an accumulation of these capsid proteins in the nucleus (Fig. 6*a*). In a number of cells a weak cytoplasmic staining of VP1 and VP2 could also be observed (not

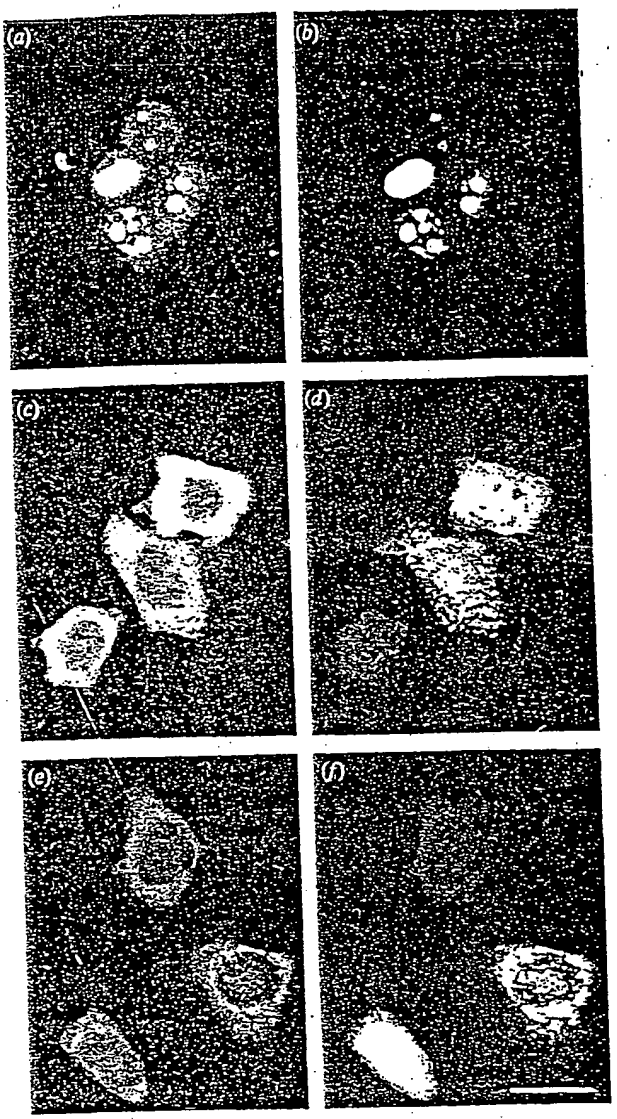

Fig. 6. Immunofluorescence analysis of wild-type and mutant capsid proteins. The subcellular localization of AAV capsid proteins in HeLa cells transfected with pTAV-2 (*a*, *b*), pTAV-p (*c*, *d*), or pTAV-d (*e*, *f*) and infected with adenovirus-2 was detected by indirect immunofluorescence using a polyclonal VP antiserum (*a*, *c*, *e*) and a monoclonal antibody A69 recognizing VP1 and VP2 only (*b*, *d*, *e*). Note the predominantly cytoplasmic, granular staining of the mutated capsid proteins. Bar marker represents 20 μm.

shown). When cells were fixed 24 h after infection with the helper virus, we typically observed a strong nucleolar staining with AAV capsid protein antibodies (Fig. 6*a* and *b*). In cells transfected with the mutant plasmids the capsid proteins were detected in the cytoplasm predominantly, often in a granular pattern, sometimes with a preferential localization close to the nuclear membrane (Fig. 6*c* to *f*). Formation of such granular VP aggregates seemed to be more prominent in cells transfected with pTAV-d (Fig. 6*e* and *f*) than in those transfected with

pTAV-p (Fig. 6*c* and *d*). Strikingly, no nucleolar staining was observed in cells transfected with the mutant plasmids at any time point although some capsid protein was detectable in the nucleus.

Discussion

We have re-examined the AAV-VP ORF in the course of the generation of viral capsid mutants which we started to develop based on a predicted RGD integrin-binding motif. DNA sequencing of two independent AAV-2 clones suggested, in addition to several other nucleotide changes, a deletion of C at position 4227 which causes a frameshift and extension of the VP ORF by 27 amino acids. This change in the VP amino acid sequence has been confirmed directly by sequencing of protease-generated peptides isolated from baculovirus-expressed VP3 protein. The DNA used for expression of VP3 was obtained from pTAV-2. The M_r of VP3 expressed in insect cells and derived from pTAV-2 is identical to that of VP3 derived from HeLa cells infected with both AAV-2 strain H (ATCC) and adenovirus (Ruffing *et al.*, 1992). This suggests that the AAV wild-type virus DNA does not contain the C-terminal ORF established by Srivastava *et al.* (1983), since the M_r difference in the capsid proteins between the baculovirus-expressed and the AAV-derived protein should have been observed. Therefore these peptide sequences demonstrate that the AAV capsid contains no RGD motif which could be involved in binding to integrins and viral uptake.

The two capsid mutants that we generated affect this newly established C-terminal sequence. In the mutant pTAV-d this sequence is deleted in addition to the previously predicted RGD and in pTAV-p I^{480} is changed to S. Both mutants showed no detectable ssDNA accumulation in spite of normal levels of AAV DNA replication. This is probably due to reduced or missing capsid protein oligomerization which correlates with a drastic cellular mislocalization of the mutated capsid proteins in comparison to the wild-type. These mutations are localized in the C terminus of the capsid proteins and affect the ORF of all three capsid proteins. Therefore they cannot be compared with mutations of individual capsid proteins in the N terminus of the capsid proteins (Muralidhar *et al.*, 1994) which also lead to defects in ssDNA accumulation and production of infectious virus.

Our findings suggest that reduced particle formation and ssDNA accumulation of the capsid protein mutants pTAV-p and pTAV-d might be a result of the mislocalization of the mutated proteins. The higher degree of mislocalization of the deletion mutant (pTAV-d; Fig. 6*e* and *f*) correlates with the lower amount of particles in the cell lysate and the complete lack of infectivity compared with the mutant pTAV-p. Based on sequence comparisons, the carboxy-terminal mutations should not affect any nuclear localization sequences in the capsid proteins. It has been shown that VP1 and VP2 are able to accumulate in the nucleus (see also Fig. 6*b*) whereas VP3 equilibrates between nucleus and cytoplasm, consistent with the positioning of nuclear accumulation sequences in the amino terminus of the capsid proteins (Ruffing *et al.*, 1992). The reduced nuclear accumulation of the capsid proteins might thus be explained rather by a conformational change of the capsid proteins that leads to cytoplasmic retention due to interaction with immobilized cytoplasmic components or due to irregular aggregation of the capsid proteins. This explanation is supported by the granular distribution pattern of the mutated capsid proteins in the cytoplasm (Fig. 6*c* to *f*) and the lack of soluble but sedimentable capsids (Fig. 5*b*). Alternatively, the interaction of the capsid proteins with a cytoplasmic component necessary for cotransport into the nucleus, could be disturbed by the C-terminal mutations. Such an interpretation would also explain the loss of nucleolar accumulation of the mutated capsid proteins despite the presence of some capsid protein in the nucleus. In any case, the observed defect in viral assembly correlates with an incomplete nuclear accumulation of the capsid proteins and a lack of transient nucleolar localization. Based on the presented data, it cannot be decided whether the mislocalization of the capsid proteins is a cause or a consequence of the assembly defect. Direct analysis of capsid protein interactions is needed to clarify the biochemical consequences of the introduced capsid protein mutations. It is clear from these data, however, that the corrected C terminus of the capsid proteins, accounting for about 10% of the total capsid amino acid sequence, is important for the generation of infectious virus.

We thank K. Berns for the plasmid pSM620, H. zur Hausen for continuous support and A. Bürkle, M. Pawlita and S. Weger for critical reading of the manuscript. We are grateful to U. Ackermann and A. Kern for excellent technical assistance.

References

Becerra, S. P., Rose, J. A., Hardy, M., Baroudy, B. M. & Anderson, C. W. (1985). Direct mapping of adeno-associated virus proteins B and C: a possible ACG initiation codon. *Proceedings of the National Academy of Sciences, U.S.A.* 82, 7919–7923.

Becerra, S. P., Koczot, F., Fabish, P. & Rose, J. A. (1988). Synthesis of adeno-associated virus structural proteins requires both alternative mRNA splicing and alternative initiations from a single transcript. *Journal of Virology* 62, 2745–2754.

Berns, K. I. & Bohenzky, R. A. (1987). Adeno-associated virus: an update. *Advances in Virus Research* 32, 243–306.

Berns, K. I. (1990). Parvovirus replication. *Microbiological Reviews* 54, 316–329.

Cassinotti, P., Weitz, M. & Tratschin, J.-D. (1988). Organization of the adeno-associated virus (AAV) capsid gene: mapping of a minor spliced mRNA coding for virus capsid protein 1. *Virology* 167, 176–184.

Chen, C. & Okayama, H. (1987). High-efficiency transformation of

mammalian cells by plasmid DNA. *Molecular and Cellular Biology* 7, 2745–2752.

CHEJANOVSKY, N. & CARTER, B. (1989). Mutagenesis of an AUG codon in the adeno-associated rep gene: effects on viral DNA replication. *Virology* 173, 120–128.

FOX, G., PARRY, N. R., BARNETT, P. V., MCGINN, B., ROWLANDS, D. J. & BROWN, F. (1989). The cell attachment site on foot-and-mouth disease virus includes the amino acid sequence RGD (arginine-glycine-aspartic acid). *Journal of General Virology* 70, 625–637.

HARLOW, E. & LANE, D. (1988). Immunoblotting. In *Antibodies. A Laboratory Manual*, pp. 471–511. Edited by E. Harlow & D. Lane. New York: Cold Spring Harbor.

HEILBRONN, R., BÜRKLE, A., STEPHAN, S. & ZUR HAUSEN, H. (1990). The adeno-associated rep gene suppresses herpes simplex virus-induced DNA amplification. *Journal of Virology* 64, 3012–3018.

HERMONAT, P. L., LABOW, M. A., WRIGHT, R., BERNS, K. I. & MUZYCZKA, N. (1984). Genetics of adeno-associated virus: isolation and preliminary characterization of adeno-associated virus type 2 mutants. *Journal of Virology* 51, 329–339.

HYNES, R. O. (1992). Integrins: versatility, modulations, and signaling in cell adhesion. *Cell* 69, 11–25.

JANIK, J. E., HUSTON, M. M. & ROSE, J. A. (1984). Adeno-associated virus proteins: origin of the capsid components. *Journal of Virology* 52, 591–597.

LAEMMLI, U. K. (1970). Cleavage of structural proteins during the assembly of the head of bacteriophage T4. *Nature. London* 227, 680–685.

LAUGHLIN, C. A., TRATSCHIN, J., COON, H. & CARTER, B. J. (1983). Cloning of infectious adeno-associated virus genomes in bacterial plasmids. *Gene* 23, 65–73.

MENDELSON, E., TREMPE, J. P. & CARTER, B. J. (1986). Identification of trans-active Rep proteins of adeno-associated virus by antibodies to a synthetic oligopeptide. *Journal of Virology* 60, 823–832.

MUZYCZKA, N. (1992). Use of adeno-associated virus as a general transduction vector for mammalian cells. *Current Topics in Microbiology and Immunology* 158, 97–129.

MURALIDHAR, S., BECERRA, S. P. & ROSE, J. A. (1994). Site-directed mutagenesis of adeno-associated virus type 2 structural protein initiation codons: effects on regulation of synthesis and biological activity. *Journal of Virology* 68, 170–176.

MYERS, M. W. & CARTER, B. J. (1980). Assembly of adeno-associated virus. *Virology* 102, 71–82.

MYERS, M. W. & CARTER, B. J. (1981). Adeno-associated virus replication. *Journal of Biological Chemistry* 265, 567–570.

REDEMANN, B. E., MENDELSON, E. & CARTER, B. J. (1989). Adeno-associated virus Rep protein synthesis during productive infection. *Journal of Virology* 63, 873–882.

ROIVAINEN, M., HYYPIA, T., PIIRAINEN, L., KALKKINEN, N., STANWAY, G. & HOVI, T. (1991). RGD-dependent entry of coxsackievirus A9 into host cells and its bypass after cleavage of VP1 protein by intestinal proteases. *Journal of Virology* 65, 4735–4740.

RUFFING, M., ZENTGRAF, H. & KLEINSCHMIDT, J. A. (1992). Assembly of viruslike particles by recombinant structural proteins of adeno-associated virus type 2 in insect cells. *Journal of Virology* 66, 6922–6930.

RUOSLAHTI, E. & PIERSCHBACHER, M. D. (1986). Arg-Gly-Asp: a versatile cell recognition signal. *Cell* 44, 517–518.

RUOSLAHTI, E. & PIERSCHBACHER, M. D. (1987). New perspectives in cell adhesion: RGD and integrins. *Science* 238, 491–497.

SAMULSKI, R. J., BERNS, K. I., TAN, M. & MUZYCZKA, N. (1982). Cloning of adeno-associated virus into pBR322: rescue of intact virus from recombinant plasmid in human cells. *Proceedings of the National Academy of Sciences, U.S.A.* 79, 2077–2081.

SANGER, F., NICKLEN, S. & COULSON, A. R. (1977). DNA sequencing with chain-terminating inhibitors. *Proceedings of the National Academy of Sciences, U.S.A.* 74, 5463–5467.

SMUDA, J. W. & CARTER, B. J. (1991). Adeno-associated viruses having nonsense mutations in the capsid genes: growth in mammalian cells containing an inducible amber suppressor. *Virology* 184, 310–318.

SRIVASTAVA, A., LUSBY, E. W. & BERNS, K. I. (1983). Nucleotide sequence and organization of adeno-associated virus 2 genome. *Journal of Virology* 45, 555–564.

TAYLOR, J. W., OTT, J. & ECKSTEIN, F. (1985). The rapid generation of oligonucleotide-directed mutations at high frequency using phosphothioate-modified DNA. *Nucleic Acids Research* 13, 8765–8785.

THOMAS, J. O. & KORNBERG, R. D. (1975). An octamer of histones in chromatin and free in solution. *Proceedings of the National Academy of Sciences, U.S.A.* 72, 4350–4354.

TRATSCHIN, J.-D., MILLER, I. L. & CARTER, B. J. (1984). Genetic analysis of adeno-associated virus: properties of deletion mutants constructed *in vitro* and evidence for an adeno-associated virus replication function. *Journal of Virology* 51, 611–619.

(*Received 16 May 1994; Accepted 29 July 1994*)

EXHIBIT 5

JOURNAL OF VIROLOGY, Sept. 2000, p. 8635–8647 Vol. 74, No. 18
0022-538X/00/$04.00+0

Mutational Analysis of the Adeno-Associated Virus Type 2 (AAV2) Capsid Gene and Construction of AAV2 Vectors with Altered Tropism

PEI WU,[1,2] WU XIAO,[2,3] THOMAS CONLON,[2,4] JEFFREY HUGHES,[2,3] MAVIS AGBANDJE-McKENNA,[5,6,7] THOMAS FERKOL,[8] TERENCE FLOTTE,[1,2,4] AND NICHOLAS MUZYCZKA[1,2,6]*

Department of Molecular Genetics and Microbiology,[1] Department of Pediatrics,[4] Department of Molecular Pharmaceutics,[3] Department of Biochemistry,[5] Powell Gene Therapy Center,[2] UF Brain Institute,[6] and Center for Structural Biology,[7] University of Florida, Gainesville, Florida 32610-0266, and Division of Pediatric Pulmonology, Rainbow Babies and Children's Hospital, Cleveland, Ohio 44106-6006[8]

Received 1 March 2000/Accepted 8 June 2000

Adeno-associated virus type 2 (AAV2) has proven to be a valuable vector for gene therapy. Characterization of the functional domains of the AAV capsid proteins can facilitate our understanding of viral tissue tropism, immunoreactivity, viral entry, and DNA packaging, all of which are important issues for generating improved vectors. To obtain a comprehensive genetic map of the AAV capsid gene, we have constructed 93 mutants at 59 different positions in the AAV capsid gene by site-directed mutagenesis. Several types of mutants were studied, including epitope tag or ligand insertion mutants, alanine scanning mutants, and epitope substitution mutants. Analysis of these mutants revealed eight separate phenotypes. Infectious titers of the mutants revealed four classes. Class 1 mutants were viable, class 2 mutants were partially defective, class 3 mutants were temperature sensitive, and class 4 mutants were noninfectious. Further analysis revealed some of the defects in the class 2, 3, and 4 mutants. Among the class 4 mutants, a subset completely abolished capsid formation. These mutants were located predominantly, but not exclusively, in what are likely to be β-barrel structures in the capsid protein VP3. Two of these mutants were insertions at the N and C termini of VP3, suggesting that both ends of VP3 play a role that is important for capsid assembly or stability. Several class 2 and 3 mutants produced capsids that were unstable during purification of viral particles. One mutant, R432A, made only empty capsids, presumably due to a defect in packaging viral DNA. Additionally, five mutants were defective in heparan binding, a step that is believed to be essential for viral entry. These were distributed into two amino acid clusters in what is likely to be a cell surface loop in the capsid protein VP3. The first cluster spanned amino acids 509 to 522; the second was between amino acids 561 and 591. In addition to the heparan binding clusters, hemagglutinin epitope tag insertions identified several other regions that were on the surface of the capsid. These included insertions at amino acids 1, 34, 138, 266, 447, 591, and 664. Positions 1 and 138 were the N termini of VP1 and VP2, respectively; position 34 was exclusively in VP1; the remaining surface positions were located in putative loop regions of VP3. The remaining mutants, most of them partially defective, were presumably defective in steps of viral entry that were not tested in the preliminary screening, including intracellular trafficking, viral uncoating, or coreceptor binding. Finally, in vitro experiments showed that insertion of the serpin receptor ligand in the N-terminal regions of VP1 or VP2 can change the tropism of AAV. Our results provide information on AAV capsid functional domains and are useful for future design of AAV vectors for targeting of specific tissues.

Adeno-associated virus type 2 (AAV2) belongs to the human parvovirus family, which requires a helper virus for productive replication (5, 7, 8). The nonenveloped capsid adopts an icosahedral structure with a diameter of approximately 20 nm. Packaged within the capsid is a single-stranded DNA genome of 4.7 kb that contains two large open reading frames (ORFs), *rep* and *cap* (35). Three structural proteins, designated VP1, VP2, and VP3, are encoded in the *cap* ORF and made from the p40 promoter by use of alternative splicing and alternative start codons. The three proteins share the same ORF and end at the same stop codon. The C-terminal regions common to all three capsid proteins fold into a β-barrel structure that is present in several viruses (31). Their molecular masses are 87, 73, and 62 kDa, and their relative abundances within the capsid are approximately 5, 5, and 90%, respectively (26). Recently, AAV has attracted a significant amount of interest as a vector for gene therapy (6, 26). It has a number of unique advantages that are potentially useful for gene therapy applications, including the ability to infect nondividing cells, a lack of pathogenicity, and the ability to establish long-term gene expression.

Early genetic studies on deletion mutants of AAV revealed that capsid proteins were required for accumulation of single-stranded DNA and production of infectious particles (19, 38). Mutations in the C-terminal region common to all three proteins also abolished virion formation and failed to accumulate single-stranded DNA (32). VP1 was thought to be important for virus infectivity or stability because mutations in the N-terminal region unique to VP1 produced DNA-containing particles with significantly reduced infectivity (19, 38). In vitro

* Corresponding author. Mailing address: Department of Molecular Genetics and Microbiology, P.O. Box 100266, College of Medicine, University of Florida, Gainesville, FL 32610. Phone: (352) 392-5913. Fax: (352) 392-5914. E-mail: muzyczka@mgm.ufl.edu.

assembly studies (33) and capsid initiation codon mutagenesis studies (25) suggested that both VP2 and VP3 were required for capsid formation and production of infectious particles, and either VP1 or VP2 was required for nuclear localization of VP3. Recently, Hoque et al. (19b) have shown that the VP2 N-terminal residues 79 to 34 are sufficient for nuclear translocation and suggested that the major function of VP2 is to translocate VP3 into the nucleus. A recent insertional mutation study on AAV capsid protein revealed that mutations in the capsid gene could affect AAV capsid assembly and infection (30). Since the crystal structure of AAV was still unavailable, the functional domains of the AAV capsid proteins were mostly predicted based on information derived from other related autonomous parvoviruses, canine parvovirus (CPV), feline panleukopenia virus, and B19, whose crystal structures were available (1, 2, 40, 41). Sequence comparison of AAV to these viruses revealed a few conserved functional domains (9, 10), but the exact functions of these domains were not clear.

While certain groups of cells cannot be transduced by AAV (22, 27), AAV can transduce a wide variety of tissues, including brain, muscle, liver, lung, vascular endothelial, and hematopoietic cells (12–14, 16, 21, 45, 48). Recently, Summerford and Samulski (37) reported that heparan sulfate proteoglycan is the primary cellular receptor for AAV, and their group further revealed that the binding site lies within VP3 (30). In addition, human fibroblast growth factor receptor 1 and $\alpha_v\beta_5$ integrin were identified as coreceptors for AAV (28, 36). Attempts to alter the AAV capsid also have been made in order to expand the tropism of AAV. Yang et al. (47) showed improved infectivity of hematopoietic progenitor cells by generating a chimeric recombinant AAV (rAAV) having the single-chain antibody against human CD34 protein. Girod et al. (15) showed that insertion of the L14 epitope into the capsid coding region can expand the tropism of this virus to cells nonpermissive for AAV infection that bear the L14 receptor. However, in both cases the normal AAV tropism was not disrupted. Ideally, for the purpose of retargeting, the normal AAV receptor binding would need to be modified so that rAAV infects only targets bearing the receptors for the engineered epitope.

In this study, we used site-directed mutagenesis to mutate the capsid ORF. Initially, 48 alanine scanning mutations were made in which two to five charged amino acids in the AAV capsid ORF were mutated to alanine residues by site-directed mutagenesis. We reasoned that since the mutations were an average of 15 to 20 amino acids (aa) apart and spanned the whole capsid gene, some of them would inevitably fall in or near the functional domains of AAV capsid. In addition, over 40 substitution and insertion mutations were made in a search for regions that could tolerate insertions for the purpose of retargeting AAV vectors. By analyzing these mutants, we obtained a preliminary functional map of the AAV capsid protein. Our results identified critical regions within the capsid that were potentially responsible for receptor binding, DNA packaging, capsid formation, and infectivity. In addition, we identified sites that were suitable for epitope insertions that might be useful for targeted gene delivery.

MATERIALS AND METHODS

Cell culture. Low-passage-number (passages 27 to 38) HFK 293 cells (17) and HeLa cells were grown in Dulbecco's modified Eagle's medium supplemented with 10% fetal calf serum, penicillin (100 U/ml), and streptomycin (100 U/ml) at 37°C and 5% CO_2. IB3 cells were propagated as described elsewhere (34).

Construction of AAV capsid mutant plasmids. Plasmid pIM45 (previously called pIM29-45 [23]) was used as the template for all mutant constructions. Mutagenesis was achieved by using the Stratagene site-directed mutagenesis kit according to the supplier's manual. For each mutant, we designed two PCR primers which contained the sequence of alanine substitution or insertion plus a unique endonuclease restriction site flanked by 15 to 20 homologous bp on each side of the substitution or insertion. The restriction site was designed to facilitate subsequent DNA sequencing of the mutants and for potential insertion of tags or foreign epitopes. The PCR products were digested with endonuclease *Dpn*I to eliminate the parental plasmid template and were propagated in *Escherichia coli* XL-Blue (Stratagene). Miniprep DNAs were extracted from ampicillin-resistant colonies and were screened by restriction endonuclease digestion. Positive clones were sequenced in the capsid ORF region. The capsid ORF was then subcloned back into the pIM45 backbone with *Sma*I and *Sph*I to eliminate background mutations. The same mutagenesis strategy was used for peptide substitution and insertion mutant constructions.

Production of rAAV particles. To produce rAAV with mutant capsid proteins, we transfected 293 cells with three plasmids: (i) pIM45, which supplied either wild-type (wt) or mutant capsid proteins (23); (ii) pXX6, which contained the adenovirus (Ad) helper genes (46); and (iii) pTRUF5, which contains the green fluorescent protein (*gfp*) gene driven by the cytomegalovirus (CMV) promoter and flanked by the AAV terminal repeats (22). In some experiments, pTRUF5 was substituted with CBA-AT, a recombinant AAV plasmid that contains the human α1-antitrypsin (hAAT) gene under the control of the CMV–β-actin promoter. The plasmids were mixed at a 1:1:1 molar ratio. Plasmid DNAs used for transfection were purified by the QIAGEN Maxi-prep kit according to the supplier's manual.

The transfections were carried out as follows. 293 cells were split 1:2 the day before the transfection so that they could reach 75% confluency the next day. Ten 15-cm-diameter plates were transfected at 37°C, using calcium phosphate as described elsewhere (51), and incubated at 37°C. Forty-eight hours after transfection, cells were harvested by centrifugation at 1,140 × *g* for 10 min, the pellets were resuspended in 10 ml of lysis buffer (0.15 M NaCl, 50 mM Tris-HCl [pH 8.5]), and viruses were released by freezing and thawing three times. The crude rAAV lysates were treated with Benzonase (pure grade; Nycomed Pharma A/S) at a final concentration of 50 U/ml at 37°C for 30 min. The crude lysates were clarified by centrifugation at 3,700 × *g* for 20 min, and the supernatant was subjected to further purification by iodixanol step gradient and heparan sulfate affinity purification as previously described (51).

To determine whether any of the mutants were temperature sensitive, the transfections were done in six-well dishes as duplicates at 39.5 and 32°C. Viruses were resuspended in 250 μl of lysis buffer. All crude rAAV preparations were stored at −80°C until their titers were determined.

Gel electrophoresis, immunoblotting, and immunoprecipitation. Crude or purified rAAV samples were analyzed on sodium dodecyl sulfate (SDS)–10% polyacrylamide gels. The samples were mixed with sample buffer and boiled at 100°C for 5 min before loading. For immunoblotting, the proteins were transferred to a Nitro-bond membrane at 4°C, and the membrane was probed with monoclonal antibody (MAb) B1, directed against the capsid proteins (43). The capsid bands were visualized by peroxidase-coupled secondary antibodies using ECL (enhanced chemiluminescence detection) (Amersham) as suggested by the supplier.

For immunoprecipitation, heparan column-purified rAAV samples were diluted in 10 volumes of NETN buffer (0.1 M NaCl, 1 mM EDTA, 20 mM Tris-HCl [pH 7.5], 0.5% Nonidet P-40) and incubated overnight at 4°C in the presence of a MAb to the hemagglutinin (HA) epitope conjugated to Sepharose beads (BAbCo). For a negative control, MAb AU1-conjugated beads (BAbCo) were used. AU1 is a commonly used epitope, DTYRYI. After incubation, the samples were centrifuged for 5 min at 17,600 × *g* at 4°C. The beads were washed three times with 1 ml of NETN for 10 min at room temperature and resuspended in protein loading buffer. After centrifugation, the supernatant was precipitated with 15% trichloroacetic acid on ice for 1 h and centrifuged for 45 min at 4°C, and the pellet was resuspended in loading buffer. The samples then were boiled in sample buffer and analyzed by Western blotting with MAb B1 as described above.

Virus titers. The infectious titers of rAAV-containing wt and mutant capsids were measured at two temperatures, 39.5 and 32°C, for the alanine scanning mutants and at 37°C for all other mutants by using the fluorescent cell assay, which detects expression of the *gfp* gene. This was done essentially as described previously by Zolotukhin et al. (51). Briefly, 293 cells were seeded in a 96-well dish the day before infection so that they would reach about 75% confluence the next day. Serial dilutions of wt and mutant rAAV-GFP crude preparations were added to the cells in the presence of Ad5 at a multiplicity of infection (MOI) of 10. The cells and viruses were incubated at 37°C (or 32° and 39.5°C) for 48 h, and the titers were determined by counting the number of green cells with the fluorescence microscope. For each mutant, the infections were done twice and the average was taken. For mutants that contained a packaged CBA-AT gene, infectivity was measured by the infectious center assay on 293 cells as previously described (51) and by enzyme-linked immunosorbent assay (ELISA) measurement of hAAT secreted into culture media from infected cells as described elsewhere (34).

To determine the rAAV physical particle titer, we used the A20 ELISA kit (American Research Bioproducts). The crude rAAV stocks were serially diluted and incubated with the A20 kit plate. The readings that fell into the linear range were taken, and the titers were read off the standard according to the manufacturer's instructions. The A20 antibody detects both full and empty particles (44).

To determine the titer of rAAV physical particles that were full (i.e., contained

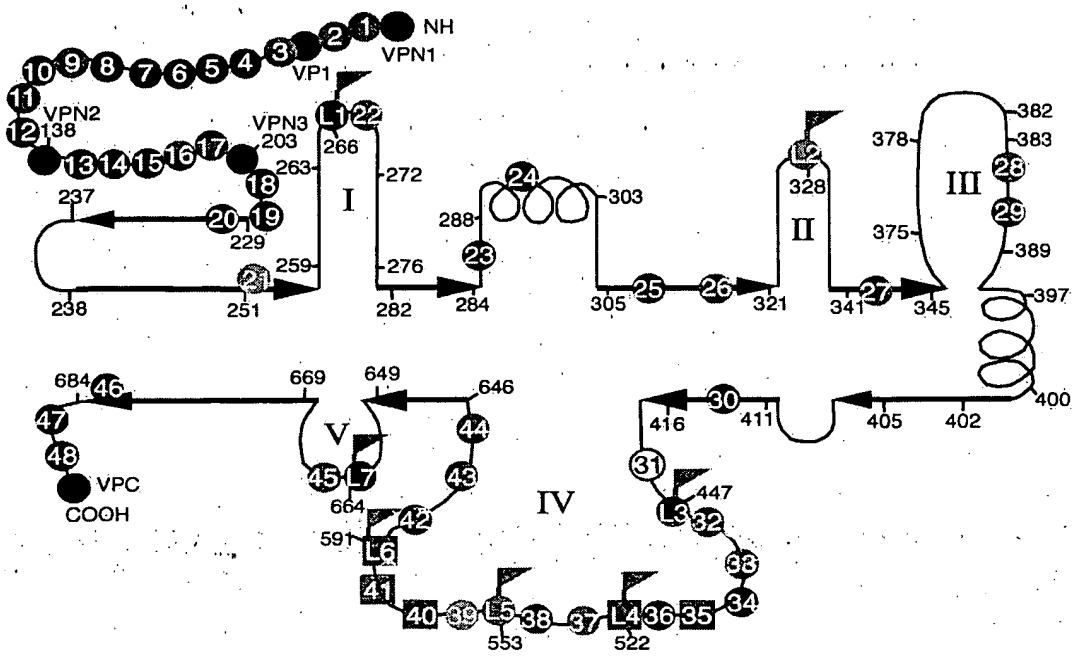

FIG. 1. Distribution of alanine scanning and HA epitope insertion mutants. Positions of the alanine scanning mutants (colored circles or squares) and the HA insertion mutants (flagged circles or squares) are shown on a diagram of the putative secondary structure of the AAV capsid protein adapted from a comparison of parvovirus capsid sequences by Chapman and Rossmann (9). Some important amino acid positions and mutant positions are illustrated by numbers with short lines. Heavy arrows represent putative β sheets, and helices represent putative α helices. The five putative loop regions are numbered I to V. The colors of the circles indicate the phenotypes of the mutants as shown below:

Class	Mutant(s)	Color	Primary phenotype	Defect
1	*mut*1, *mut*2, *mut*3, *mut*9, *mut*11, *mut*13, *mut*14, *mut*16, *mut*17, *mut*29, *mut*32, *mut*38, *mut*43, *mut*44, *mut*45	Red	Wild type	
2a	*mut*4, *mut*5, *mut*6, *mut*7, *mut*8, *mut*10, *mut*12, *mut*15, *mut*18, *mut*30, *mut*34, *mut*36, *mut*48; L1, L3, L7, VPN1, VP1, VPN2	Blue	Partially defective	
2b	*mut*21, *mut*39	Light blue	Partially defective	Unstable capsid
2c	*mut*41, L6	Purple	Partially defective	Heparan binding negative
3a	*mut*26, *mut*27, *mut*28, *mut*33	Green	Temperature sensitive	
3b	*mut*35	Purple	Temperature sensitive	Heparan binding negative
4a	*mut*22, *mut*37; L5, L2	Brown	Noninfectious	
4b	*mut*19, *mut*20, *mut*23, *mut*24, *mut*25, *mut*42, *mut*46, *mut*47; VPN3, VPC	Black	Noninfectious	No capsid made
4c	*mut*31	White	Noninfectious	Empty capsid
4d	*mut*40, L4	Purple	Noninfectious	Heparan binding negative

DNA), we used the quantitative competitive PCR (QC-PCR) assay as described previously (51). The crude rAAV stocks (100 μl) were digested first with DNase I to eliminate contaminating unpackaged DNA in 50 mM Tris-HCl (pH 7.5)–10 mM $MgCl_2$ for 1 h at 37°C and then incubated with proteinase K (Boehringer) in 10 mM Tris HCl (pH 8.0)–10 mM EDTA–1% SDS for 1 h at 37°C. Viral DNA was extracted twice in phenol-chloroform and once with chloroform and then precipitated by ethanol in the presence of glycogen (10%). The DNA was washed with ethanol, dried, and dissolved in 100 μl of H_2O, and 1 μl of the viral DNA was used for QC-PCR. Serial dilutions of the internal standard plasmid DNA with a deletion of GFP were included in the reaction, and the PCR products were separated by 2% agarose gel electrophoresis. The densities of the target and competitor bands in each lane were measured using ZERO-Dscan image analysis system software (version 1.0; Scanalytics) to determine the DNA concentration of the virus stock.

Heparan column binding assay. The ability of mutants to bind to heparan sulfate was tested essentially as previously described (51). Crude rAAV preparations containing wt or mutant capsids were first subjected to iodixanol gradient purification. The 40% layer was then collected and loaded onto a 1-ml preequilibrated heparan column at room temperature (immobilized on cross-linked 4% beaded agarose; Sigma H-6508). The flowthrough fraction, wash (3 column volumes), and 1 M NaCl eluate were collected, and equivalent amounts of each sample were mixed with SDS sample buffer and electrophoresed on SDS-polyacrylamide gels. The yield of capsid proteins in each fraction was monitored with MAb B1 by Western blotting and ECL detection.

EM. Electron microscopy (EM) was done in the ICBR EM lab of the University of Florida. Iodixanol gradient and heparan column-purified wt or mutant GFP-rAAVs were desalted and concentrated by using a Centricon 10 filter (Amicon). About a 5-μl drop of the virus sample was spotted onto carbon-coated grids and left for 1 min at room temperature. Excess fluid was drawn off, and the sample was washed three times with phosphate-buffered saline; 5 μl of 1% uranyl acetate was added for 10 s, and the grid was dried at room temperature for 10 min before viewing under EM.

RESULTS

Generation of AAV capsid mutations. We began our studies by using alanine scanning site-directed mutagenesis in the hope that some of the mutants would be temperature sensitive (11). The mutants were constructed in the noninfectious AAV plasmid, pIM45, which contains all of the AAV DNA sequence except the AAV terminal repeats. There are approximately 60 charged clusters in the AAV capsid gene. Some of the clusters are overlapping; in those cases, only one cluster was chosen. For the initial round of mutagenesis, 48 sites, named *mut*1 to *mut*48, were targeted. These were spaced approximately equally over the capsid gene, with 12 mutants exclusively in VP1, 5 in VP2, and the rest in VP3 (Fig. 1). With the exceptions noted below, in each cluster, all charged amino acids were converted to alanine. The mutations were created so that they also contained a restriction site at the site of mutation to

facilitate confirmation of the mutant sequence and subsequent insertion of foreign epitopes (Table 1). In addition, after sequence comparison of AAV serotypes 1 to 6, several other positions were targeted. *mut*28 and *mut*35 were made at positions where extra amino acids were found in AAV4 by sequence comparison with AAV2. *mut*32 was made by replacing TTT with AAA since TTT was not conserved among other AAV serotypes at aa 454. Finally, in *mut*29 and *mut*31, only one Arg residue was changed to Ala, and in *mut*45 and *mut*48, only one Lys was changed to Ala. The positions of the alanine scanning mutants and the specific amino acid substitutions are summarized in Table 1 and Fig. 1.

Infectious titer assays reveal four general classes of mutants. To determine the effect of each mutation on viral infectivity, we used either wt pIM45 or a mutant pIM45 plasmid to complement the growth of pTRUF5. pTRUF5 is a recombinant AAV plasmid that contains the *gfp* gene under the control of a CMV enhancer-promoter (22). The resulting recombinant TRUF5 virus contained either wt or mutant capsid proteins and could be titered for infectivity by counting green fluorescent cells in the presence of an Ad5 coinfection. We had shown previously that the fluorescent cell assay produced titers within two- to threefold of those obtained with a conventional infectious center assay (51). Initially, each mutant was grown and titered at either 39.5 or 32°C to determine if any of the mutants were temperature sensitive. The experiments were done twice, and there was no significant variation in titer. On the basis of these titers, the mutants could be grouped into four classes (Fig. 2; Table 1). Class 1 contained mutants that have an infectious titer similar to the wt titer (less than 1 log difference; for example, *mut*1 and *mut*2). Class 2 contained partially defective mutants with infectious titers 2 to 3 logs lower than the wt titer (for example, *mut*4 and *mut*5). Class 3 contained temperature-sensitive mutants; three of these (*mut*26, *mut*27, and *mut*33) were heat sensitive, and two (*mut*28 and *mut*35) were cold sensitive. Class 4 consisted of 12 noninfectious mutants, whose titers were more than 5 logs lower than the wt titer.

Noninfectious (class 4) mutants and temperature-sensitive (class 3) mutants were defective in packaging DNA or in forming stable virus particles. To determine the probable causes for the different defective mutants, we focused first on class 3 and 4 mutants. For convenience, we ignored the fact that the temperature-sensitive mutants had low infectivity when grown at the partially restrictive temperature of 37°C (data not shown), and viral preparations for all class 3 and 4 mutants were made at 37°C. To determine if these mutants were able to make capsids, we used the A20 ELISA. The A20 antibody recognizes only intact AAV particles (43) and is useful for determining the physical particle titer irrespective of whether the capsids contain DNA (18). Eight of sixteen mutants that were tested were negative by ELISA reading (Table 2), indicating that they were unable to make capsids or that the capsids were unstable even in crude lysate preparations. All of these were class 4 (noninfectious) mutants and were classified as class 4b (Table 1; Fig. 1).

QC-PCR assays also were performed on most of the class 3 and 4 mutants. The QC-PCR assay measures the titer of AAV particles that contain DNase-resistant rAAV genomes (Fig. 3). We have shown previously that it provides physical particle titers that are equivalent to those obtained by dot blot assay but has better sensitivity at low particle titers (51). As expected, mutants that were negative for the synthesis of AAV particles by A20 ELISA were also negative by QC-PCR assay (Table 2; Fig. 3). Most of the remaining mutants, which were positive for A20 particles, were also positive for packaged viral DNA in the QC-PCR assay (Fig. 3; Table 2). This group of noninfectious mutants (*mut*22 and *mut*37) were called class 4a (Table 1; Fig. 1). Their defect was not in packaging but rather in the binding, internalization, or uncoating steps of the viral entry process. One A20-positive mutant (*mut*31) was an exception in that it was A20 positive but DNA negative by QC-PCR assay. This meant that *mut*31 formed intact virus particles that were empty. To confirm this, *mut*31 was examined by EM (Fig. 4), and it did indeed make empty particles. In contrast, the partially defective class 2 mutant, *mut*4, produced particles similar to wt particles. *mut*31 was assigned to class 4c (Fig. 1; Table 1).

Some mutants are defective for binding the viral receptor. One potential cause for the reduced infectivity of class 2, 3, or 4 mutants might be that they were unable to bind the viral cell surface receptor, the first step of the infectious cycle. Heparan sulfate proteoglycan has been identified as the primary cell surface receptor for AAV (37). To test whether these mutants could bind heparan, we developed a heparan column binding assay (Materials and Methods). Iodixanol-purified wt or mutant rAAVs were passed through a heparan agarose column, and the AAV capsid proteins in the starting material and the bound (eluate) and unbound (flowthrough and wash) fractions were monitored by Western blotting using MAb B1, which recognizes all three capsid proteins (Fig. 5; Table 3). As expected, wt AAV had a high affinity for the heparan column, since little capsid protein was detected in the flowthrough and wash fractions, and most of the capsid protein was detected in the eluate. The same was true of most of the mutants tested (Fig. 5; Table 3). Two mutants, however, *mut*35 and *mut*41, bound poorly to heparan (Fig. 5). A third mutant, *mut*40, which is located about 20 aa away from *mut*41, also bound with reduced affinity (Fig. 5). This suggested that the primary defect in these mutants was their inability to bind to heparan sulfate proteoglycan. We classified *mut*35 as class 3b (temperature sensitive and heparan binding negative), *mut*41 as class 2c (partially defective and heparan binding negative), and *mut*40 as class 4d (noninfectious and heparan binding negative) (Fig. 1; and Table 1).

Three class 4b mutants, *mut*20, *mut*25, and *mut*46, could not be detected by Western analysis (Table 3). This was consistent with the fact that they made no capsid that was detectable with the A20 antibody (Table 2). Additionally, *mut*27, a temperature-sensitive mutant, and two class 2 mutants, *mut*21 and *mut*39, did not give any Western signal with MAb B1 (Fig. 5; Table 3). The heat-sensitive mutant, *mut*27, was presumably unstable at the nonpermissive temperature used for growing this virus. *mut*21 and *mut*39 were partially defective when assayed in crude extracts (Fig. 2). The fact that they could not be detected by capsid antibody after iodixanol centrifugation suggests that these capsids were also unstable during purification. These mutants were assigned to class 2b on the basis of their capsid instability (Table 1; Fig. 1). The rest of the mutants in class 2 that bind to heparan were classified as class 2a, partially defective, and heparan binding positive (Tables 1 and 3; Fig. 1). The nature of their defect was not clear but presumably was due to some step in the infectious process that occurs after viral attachment to the cell surface.

Regions tolerating alanine substitutions do not tolerate other kinds of substitutions. We wanted to determine whether the class 1 mutants defined positions in the capsid genes that were truly nonessential for capsid function. To test this, we constructed a series of mutants in which either the serpin receptor ligand, FVFLI (50), or the FLAG antibody epitope, DY KDDDDKYK, was substituted for capsid sequences at many of the class 1 mutant positions (Table 4). A number of class 2 and class 4 mutants were tried as well. The serpin substitution

TABLE 1. Summary of all mutants

Mutant[a]	Type[b]	Amino acid positions[b]	Class	Phenotype[c]
*mut*1[1]	Ala sub	9-13 DWLED-AWLAA	1	wt
*mut*2[1]	Ala sub	24-28 KLKPG-ALAPG	1	wt
*mut*3[2]	Ala sub	33-37 KPKER-APAAA	1	wt, surface
*mut*4[2]	Ala sub	39-43 KDDSR-AAASA	2a	pd, hep$^+$
*mut*5[3]	Ala sub	63-67 EPVNE-APVNA	2a	pd, hep$^+$
*mut*6[2]	Ala sub	67-71 EADAA-AAAAA	2a	pd, hep$^+$
*mut*7[2]	Ala sub	74-78 EHDKA-AHAAA	2a	pd, hep$^+$
*mut*8[2]	Ala sub	76-80 DKAYD-AAAYA	2a	pd, hep$^+$
*mut*9[1]	Ala sub	84-88 DSGDN-ASGAN	1	wt
*mut*10[2]	Ala sub	95-99 HADAE-AAAAA	2a	pd, hep$^+$
*mut*11[2]	Ala sub	102-107 ERLKED-AALAAA	1	wt
*mut*12[2]	Ala sub	122-126 KKRVL-AAAVL	2a	pd, hep$^+$
*mut*13[2]	Ala sub	142-146 KKRPV-AAAPV	1	wt
*mut*14[1]	Ala sub	152-156 EPDSS-APASS	1	wt
*mut*15[2]	Ala sub	168-172 RKRLN-AAALN	2a	pd, hep$^+$
*mut*16[2]	Ala sub	178-182 GDADS-GAAAS	1	wt
*mut*17[1]	Ala sub	180-184 DSVPD-ASVPA	1	wt
*mut*18[2]	Ala sub	216-220 EGADG-AGAAG	2a	pd, hep$^+$
*mut*19[1]	Ala sub	228-232 WHCDS-WACAS	4b	ni, no capsid
*mut*20[2]	Ala sub	235-239 MGDRV-MGAAV	4b	ni, no capsid
*mut*21[4]	Ala sub	254-258 NHLYK-NALYA	2b	pd, unstable capsid
*mut*22[4]	Ala sub	268-272 NDNHY-NANAY	4a	ni, full particle
*mut*23[4]	Ala sub	285-289 NRFHC-NAFAC	4b	ni, no capsid
*mut*24[2]	Ala sub	291-295 FSPRD-FSPAA	4b	ni, no capsid
*mut*25[2]	Ala sub	307-311 RPKRL-APAAL	4b	ni, no capsid
*mut*26[2]	Ala sub	320-324 VKEVT-VAAVT	3a	hs
*mut*27[1]	Ala sub	344-348 TDSEY-TASAY	3a	hs
*mut*28[2]	Ala ins	384-385 AAA	3a	cs
*mut*29[1]	Ala sub	389 R-A	1	wt
*mut*30[2]	Ala sub	415-419 FEDVP-FAAVP	2a	pd, hep$^+$
*mut*31[4]	Ala sub	432 R-A	4c	ni, empty particle
*mut*32[2]	Ala sub	454-456 TTT-AAA	1	wt
*mut*33[2]	Ala sub	469-472 DIRD-AIAA	3a	hs
*mut*34[2]	Ala sub	490-494 KTSAD-ATSAA	2a	pd, hep$^+$
*mut*35[2]	Ala ins	509 AAAA	3b	cs, hep$^-$, surface
*mut*36[1]	Ala sub	513-517 RDSLV-AASLV	2a	pd, hep$^+$
*mut*37[2]	Ala sub	527-532 KDDEEK-AAAAA	4a	ni, full particle
*mut*38[2]	Ala sub	547-551 SEKTN-SAATN	1	wt
*mut*39[2]	Ala sub	553-557 DIEKV-AIAAV	2b	pd, unstable capsid
*mut*40[2]	Ala sub	561-565 DEEEI-AAAAI	4d	ni, hep$^-$, full particle, surface
*mut*41[2]	Ala sub	585-588 RGNR-AGAA	2c	pd, hep$^-$, surface
*mut*42[2]	Ala sub	607-611 QDRDV-QAAAV	4b	ni, no capsid
*mut*43[2]	Ala sub	624-628 TDGHF-TAGAF	1	wt
*mut*44[1]	Ala sub	637-641 FGLKH-FGLAA	1	wt
*mut*45[2]	Ala sub	665 K-A	1	wt
*mut*46[2]	Ala sub	681-683 EIE-AAA	4b	ni, no capsid
*mut*47[2]	Ala sub	689-693 ENSKR-ASSAA	4b	ni, no capsid
*mut*48[1]	Ala sub	706 K-A	2a	pd, hep$^+$
L1	HA ins	266	2a	pd, A20$^-$, A20 epitope$^-$, surface
L2	HA ins	328	4a	ni, A20$^+$, surface
L3	HA ins	447	2a	pd, hep$^+$, surface
L4	HA ins	522	4d	ni, hep$^-$, surface
L5	HA ins	553	4a	ni, A20$^+$, surface
L6	HA ins	591	2c	pd, hep$^-$, surface
L7	HA ins	664	2a	pd, hep$^+$, surface
VPN1	HA, AU ins	1	2a	pd, hep$^+$, surface
VP1	HA ins, Ser sub	34	2a	pd, hep$^+$, surface
VPN2[d]	HA, Ser ins	138	2a	pd, hep$^+$, surface
VPN3	HA, Ser ins	203	4b	ni, no capsid
VPC	HA, Ser, AU, His ins	735	4b	ni, no capsid
*mut*1subser1	Ser sub	10	4a	ni, A20$^+$
*mut*2subser2	Ser sub	24	4a	ni, A20$^+$
*mut*3subser3	Ser sub	34	2a	pd, hep$^+$
*mut*9subser4	Ser sub	84	4a	ni, A20$^+$
*mut*14subser5	Ser sub	150	4a	ni, A20$^+$
*mut*16subser6	Ser sub	178	4b	ni, no capsid
*mut*19subser7	Ser sub	224	4b	ni, no capsid

Continued on following page

TABLE 1—*Continued*

Mutant[a]	Type[b]	Amino acid positions[b]	Class	Phenotype[c]
*mut*32subser8	Ser sub	454	4b	ni, no capsid
*mut*37subser9	Ser sub	526	4b	ni, no capsid
*mut*39subser10	Ser sub	553	4b	ni, no capsid
*mut*40subser11	Ser sub	562	4b	ni, no capsid
*mut*41subser12	Ser sub	590	4b	ni, no capsid
*mut*44subser13	Ser sub	638	4b	ni, no capsid
*mut*45subser14	Ser sub	664	4b	ni, no capsid
*mut*46subser15	Ser sub	682	4b	ni, no capsid
*mut*4subflg2	FLAG sub	39	4a	ni, $A20^+$
*mut*8subflg3	FLAG sub	76	4a	ni, $A20^+$
*mut*16subflg4	FLAG sub	178	4a	ni, $A20^+$
*mut*32subflg5	FLAG sub	454	4a	ni, $A20^+$
*mut*37subflg6	FLAG sub	526	4a	ni, $A20^+$
*mut*38subflg7	FLAG sub	547	4a	ni, $A20^+$
*mut*40subflg8	FLAG sub	562	4b	ni, no capsid
*mut*44subflg9	FLAG sub	638	4b	ni, no capsid
*mut*45subflg10	FLAG sub	664	4b	ni, no capsid
*mut*46subflg11	FLAG sub	682	4b	ni, no capsid

[a] Superscripts 1 to 4 indicate that a restriction site was introduced as a result of the alanine substitution mutation: 1, *Nhe*I; 2, *Eag*I; 3, *Hpa*I; 4, *Aha*I.

[b] Ala sub, alanine substitution mutant; Ala ins, string of alanine residues inserted after the indicated amino acid; HA, AU, His, or Ser ins, insertion of the HA, AU, His, or Ser epitope immediately after the indicated amino acid of wt cap; Ser or FLAG sub, substitution of the Ser or FLAG epitope for the wt AAV capsid sequence beginning immediately after the indicated AAV amino acid residue. Amino acid tags: HA, YPYDVPDYA; AU, DTYRYI; HIS, HHHHHH; Ser, FVFLI; FLAG, DYKDDDDK.

[c] pd, partially defective for infectivity, between 1 to 3 logs lower than wt; cs and hs, cold sensitive and heat sensitive, respectively; ni, noninfectious, 5 logs lower than wt; hep^+ mutant bound to a heparan column; hep^-, mutant did not bind to heparan sulfate; no capsid, mutant was A20 ELISA negative and MAb B1 negative; $A20^+$, mutant could be detected with A20 antibody; surface, position was present on the surface of the capsid.

[d] The serpin insertion in VPN2 was KFNKPFVFLI.

(5 aa) was the same size as the largest alanine substitutions. The FLAG epitope is highly charged, as were many of the substituted wt sequences. As expected, substitutions at class 2 (partially defective) or class 4 (nonviable) positions did not produce infectious virus (Table 4). Surprisingly, although many of the class 1 serpin or FLAG substitutions produced some physical particles detectable with the A20 antibody, only one of the substitutions, serpin at aa 34 (the *mut*3 position), produced infectious virus particles in substantial yield (Table 4). Most infectious titers were reduced by 5 logs or more, and particle titers (as judged by A20 ELISA) were reduced or undetectable as well. Thus, although modification of charged residues in class 1 mutants to alanine was permissible, these regions of the capsid were nevertheless essential for capsid formation and were sensitive to other kinds of substitutions.

Putative loop regions and the N-terminal regions of VP1 and VP2 are able to accept insertions of foreign epitopes. We also chose several other sites for insertion of foreign sequences. For

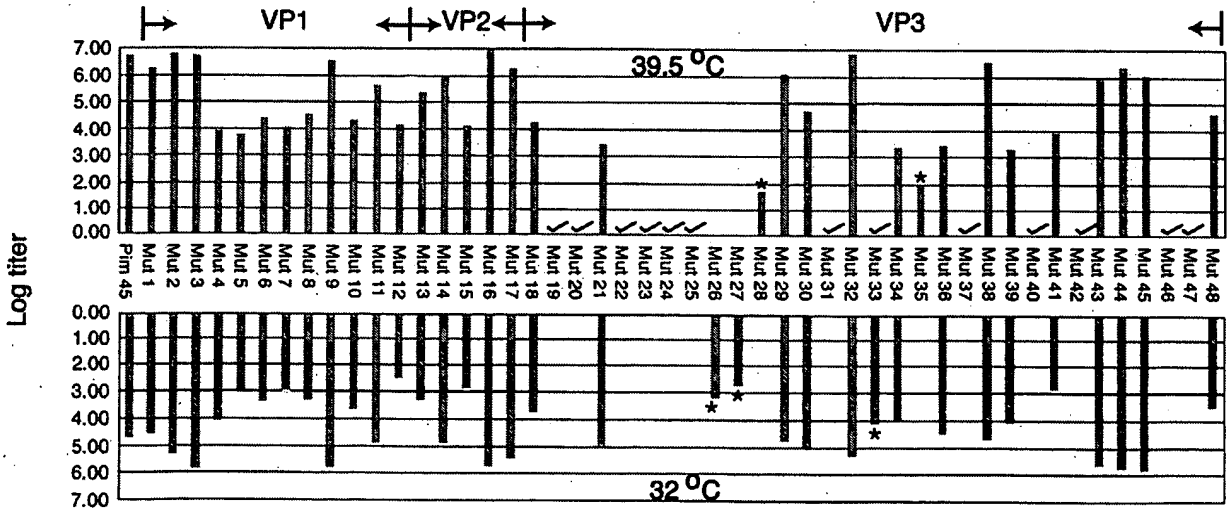

FIG. 2. Infectious titers of virus stocks containing wt and mutant capsid proteins. The GFP fluorescent cell assay was used to titer virus stocks of wt and mutant virus stocks containing the pTRUF5 genome. 293 cells were transfected with wt or mutant pIM45 complementing plasmid in the presence of pTRUF5 and pXX6 at 39.5 and 32°C. Cells were collected 48 h posttransfection and then frozen and thawed three times. The crude lysate was used to infect 293 cells at 39.5 and 32°C with Ad5 (MOI = 10). The log value of the average infectious titer (infectious particles/milliliter) that was obtained from two independent experiments is shown. There was no significant difference between experiments. The distribution of mutants unique to VP1, VP2, or VP3 is shown at the top. Asterisks indicate temperature-sensitive mutants; noninfectious mutants are indicated by check marks.

TABLE 2. Determination of physical particle titer and DNA-containing particle titer of class 2 and 3 mutants

Construct[a]	A20 ELISA[b]	QC-PCR[c]
pIM45 (wt)	+++	+++
*mut*19	−	−
*mut*20	−	−
*mut*22	++	++
*mut*23	−	−
*mut*24	−	−
*mut*25	−	−
*mut*26 (hs)	ND[d]	ND
*mut*27 (hs)	+	ND
*mut*28 (cs)	+	ND
*mut*31	++	−
*mut*33 (hs)	++	+
*mut*35 (cs)	++	++
*mut*37	++	+
*mut*40	++	++
*mut*42	−	−
*mut*46	−	ND
*mut*47	−	ND

[a] hs, heat sensitive; cs, cold sensitive.
[b] +++, $>10^{12}$ particles/ml; ++, $>10^{11}$ particles/ml; +, $>10^{10}$ particles/ml; −, $<10^{8}$ particles/ml, which was the limit of detection by A20 ELISA.
[c] +++, $>10^{11}$ full particles/ml; ++, $>10^{10}$ full particles/ml; +, $>10^{9}$ full particles/ml; −, $<10^{8}$ full particles/ml.
[d] ND, not done.

these mutants, we chose to insert the less charged HA epitope, YPVDVPDYA. The target positions for insertion were the N-terminal regions of the three capsid proteins, VP1, VP2, and VP3, the C terminus of the cap ORF and seven positions (mutants L1 to L7) that were believed to be in loop regions of the capsid protein based on an alignment of the AAV capsid sequence to that of CPV (9). Since these sites were suspected to be on the surface of the capsid, insertions at these sites might not affect capsid assembly or stability (Fig. 1). Mutations in the loop regions had been targeted successfully before by Girod et al. (15), who were able to insert the L14 ligand at aa 587 without significant loss in infectivity.

Insertions at the N termini of VP1 (VPN1) and VP3 (VPN3) and the C terminus of the cap ORF (VPC) were not well tolerated (Table 5). To eliminate the possibility that the defect in these mutants was due to the HA tag, other tags such as AU, His, and Myc were also inserted at the N termini of VP1 and VP3 and the C terminus of cap, and they also were not tolerated at those positions (Table 1 and data not shown). Insertions at three of the putative loop regions were also not viable (Table 5, mutants L2, L4, and L5). Mutants L4 (aa 522) and L5 (aa 553) were interesting in that they produced a significant yield of physical particles that were not infectious.

However, HA insertions were well tolerated at aa 34 within the N-terminal region of VP1, at the N terminus of VP2, and within three of the putative loop regions, loop I (mutant L1), loop IV (mutants L3 and L6), and loop V (mutant L7) (Table 5; Fig. 1).

Some HA insertion positions are on the capsid surface. To determine whether the HA insertion mutants contained the HA sequence exposed on the surface of the capsid, we used batch immunoprecipitation with HA MAb-conjugated beads. In each case virus was purified by iodixanol density centrifugation and heparan column chromatography to remove any soluble capsid protein that might be present in crude viral preparations. As expected, insertion of the HA tag at the N terminus of VP2 (mutant VPN2) produced a slight increase in the molecular weight of VP2 and VP1 compared to wt protein, pIM45 (Fig. 6A, B1 mAb). Western blotting with the HA MAb confirmed that the HA tag was present in both VP1 and VP2 (Fig. 6A, HA mAb). In the case of the VP1 mutant (HA insertion at aa 34 in VP1), only VP1 had a higher molecular weight and only VP1 contained the HA tag (Fig. 6A), as expected. When the viable insertions, VPN2 (HA insertion at the N terminus of VP2) and VP1 (insertion at aa 34), were treated with HA MAb-conjugated beads, substantial amounts of both viruses were precipitated (Fig. 6B, HA mAb). This demonstrated that in both cases the HA epitope was on the surface of the virus particle and accessible to the antibody. Control wt virus particles (Fig. 6B, pIM45), were not precipitated with HA MAb to any significant extent. The amount of virus in the starting material was monitored by Western blotting with B1 or HA MAb.

The putative loop HA insertion mutants, L1 to L7, were also incubated with HA MAb-conjugated beads. Although the insertions in some of these mutants produced noninfectious vi-

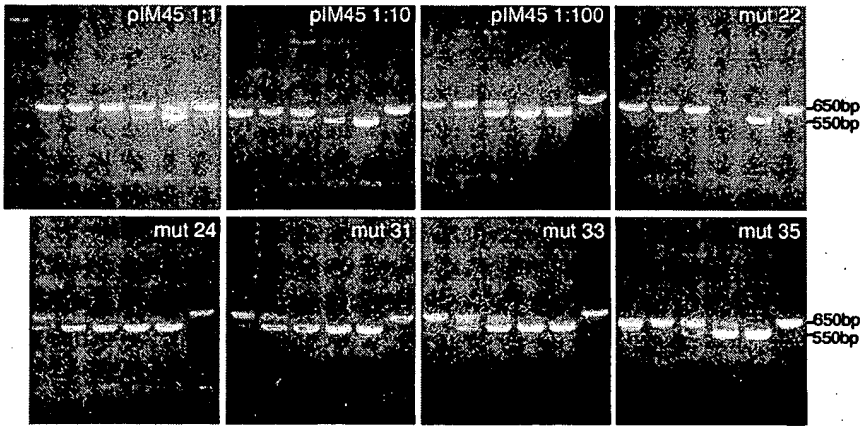

FIG. 3. QC-PCR assay of wt and mutant virus stocks to determine the DNA-containing particle titers. Crude viruses were treated with DNase to digest unpackaged DNA and then treated with proteinase K to release the packaged DNA. The viral DNA was extracted with phenol-chloroform, precipitated with ethanol, and dissolved in water. Equal amounts of viral DNA were incubated with (from left to right in each panel) 100 fg, 1 pg, 10 pg, 100 pg, 1 ng, or none of the pTRUF5 plasmid DNA containing a deletion in the *gfp* gene and amplified by PCR. The PCR products were separated on 2% agarose gels and viewed by ethidium bromide staining. The arrangement of lanes in each panel is the same. Results for wt pIM45 viral DNA at three dilutions (1:1, 1:10, and 1:100) are also shown (top left three panels). Molecular markers were included in the left lane of the top left panel.

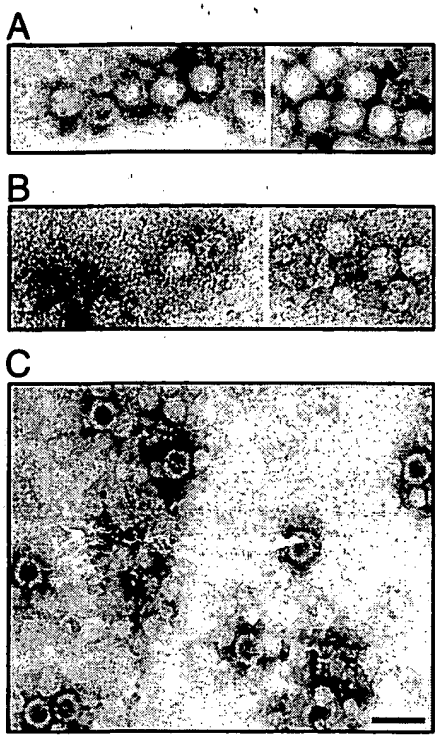

FIG. 4. EM analysis of wt (A) and mutant (*mut*4 [B] and *mut*31 [C]) rAAVs. The viruses were purified by iodixanol step gradient centrifugation and heparan column chromatography as described elsewhere (51), concentrated in a Centricon 10, and negatively stained with 1% uranyl acetate. Bar = 40 nm. Although the iodixanol step gradient might be expected to remove empty particles, these particles apparently accumulate at the 25 to 40% interface, and a significant fraction are recovered during this purification step.

rus, they all produced sufficient A20 antibody-positive virus particles to test for the presence of the HA tag on the surface of the capsid. When this was done, all of the L-series insertions were shown to be in the immunoprecipitate (bound fraction) compared to the wt (pIM45) control (Fig. 7A). This demonstrated that each of these insertions at putative loop sites resulted in the HA epitope being on the surface of the capsid.

We also checked whether these loop insertions affected heparan binding of the mutant capsids. Interestingly, two loop

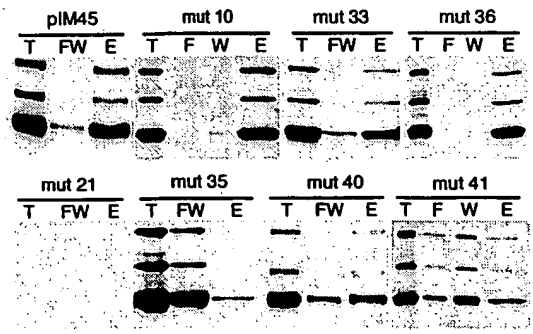

FIG. 5. Heparan binding properties of mutant viruses. Iodixanol gradient-purified virus stocks were loaded onto a heparan column. Equivalent volumes of the starting, 40% iodixanol material (T), flowthrough (F), wash (W), and eluted (E) fractions were separated on SDS–10% acrylamide gels and Western blotted with MAb B1. In some cases, the flowthrough and wash fractions were pooled (FW) and loaded together.

TABLE 3. Heparan column binding properties of class 2, 3, and 4 mutants[a]

Construct	Heparan binding	Construct	Heparan binding
pIM45	+	*mut*27	0
*mut*4	+	*mut*28	+
*mut*5	+	*mut*30	+
*mut*6	+	*mut*31	+
*mut*7	+	*mut*32	+
*mut*8	+	*mut*33	+
*mut*10	+	*mut*34	+
*mut*11	+	*mut*35	−
*mut*12	+	*mut*36	+
*mut*13	+	*mut*37	+
*mut*14	+	*mut*39	0
*mut*15	+	*mut*40	−
*mut*18	+	*mut*41	−
*mut*20	0	*mut*43	+
*mut*21	0	*mut*46	0
*mut*22	+	*mut*48	+
*mut*25	0		

[a] +, mutant virus bound to a heparan column with the same affinity as wt pIM45 virus; −, virus bound with at least a threefold-lower affinity; 0, no protein signal detected by Western blotting.

insertion mutants, L4 and L6, were found to bind heparan columns with reduced affinity (Fig. 7B), which probably accounted for the lower infectivity of these mutants in the standard fluorescent cell assay. The L4 and L6 insertions were near the heparan-binding-negative mutants *mut*35, *mut*40,

TABLE 4. Substitution of serpin or FLAG epitopes at capsid positions that tolerated alanine substitutions

Mutant	Titer[a]	
	Infectious	Physical particle
*mut*1subser1	−	+
*mut*2subser2	−	+
*mut*3subser3	1 log lower	+
*mut*9subser4	−	+
*mut*14subser5	−	+
*mut*16subser6	−	−
*mut*19subser7	−	−
*mut*32subser8	−	−
*mut*37subser9	−	−
*mut*39subser10	−	−
*mut*40subser11	−	−
*mut*41subser12	−	−
*mut*44subser13	−	−
*mut*45subser14	−	−
*mut*46subser15	−	−
*mut*4subflg2	−	+
*mut*8subflg3	−	+
*mut*16subflg4	−	+
*mut*32subflg5	−	+
*mut*37subflg6	−	+
*mut*38subflg7	−	+
*mut*40subflg8	−	−
*mut*44subflg9	−	−
*mut*45subflg10	−	−
*mut*46subflg11	−	−

[a] Either a serpin peptide sequence or the FLAG sequence was substituted for the AAV capsid sequence at the positions used previously for alanine scanning mutagenesis (Fig. 2). Infectious titers were determined by GFP fluorescent cell assay. −, infectious virus could not be detected. Physical particle titers were judged by A20 ELISA. +, particles were detectable; −, particles were not detectable.

TABLE 5. HA insertion mutants

Mutant	Position	Titer	
		Infectious[a]	Physical particle[b]
L1	aa 266	++	+
L2	aa 328	−	+
L3	aa 447	++	++
L4	aa 522	−	++
L5	aa 553	−	++
L6	aa 591	++	++
L7	aa 664	++	++
VPN1	aa 1	+	++
VP1	aa 34	+++	++
VPN2	aa 138	+++	+++
VPN3	aa 203	−	−
VPC	C terminus	−	−

[a] Determined by GFP fluorescence cell assay. +++, 1 log lower than wt; ++, 2 logs lower; +, 3 logs lower; −, at least 5 logs lower.
[b] Determined by A20 ELISA. +, 4 logs lower than wt pIM45; ++, 2 to 3 logs lower; +++, 1 log lower; −, undetectable.

and *mut*41 (Fig. 1). All five of these heparan-binding-negative mutants were located between aa 509 and 591, suggesting that this region within the AAV capsid constitutes the heparan binding domain of the capsid protein.

Changing the tropism of AAV. To determine whether we could change the tropism of rAAV by inserting a novel receptor ligand into the capsid, we constructed two mutant plasmids that contained a serpin receptor ligand. In one case the serpin ligand FVFLI (50) was substituted for the AAV capsid sequence immediately after aa 34. In the second mutant an expanded serpin receptor ligand, KFNKPFVFLI (50), was inserted at the N terminus of VP2, aa 138 (Table 1). The mutant capsid plasmids were then used to package CBA-AT, an rAAV genome that contained the hAAT gene under the control of a hybrid CMV–β-actin promoter. As seen with the HA insertion mutants described above, the serpin mutants produced rAAV viral titers that were slightly (sixfold) lower in infectivity when titered by the infectious center assay on 293 cells (data not shown). However, when equal amounts of wt or mutant virus (as determined on 293 cells) were infected into IB3 cells, both mutant viruses showed substantially higher infectivity than wt (Fig. 8). The VP2 serpin insertion was 15-fold more infectious, and the VP1 substitution mutant was approximately 62-fold more active. This suggested that IB3 cells, a lung epithelial cell line believed to express the serpin receptor, were a much better target for the serpin-tagged chimeric rAAVs than wt and that the tropism of the mutant rAAVs had been changed. Because both mutants retained the wt heparan binding region, we also infected IB3 cells in the presence of heparan sulfate to see if they continued to use heparan sulfate proteoglycan for viral

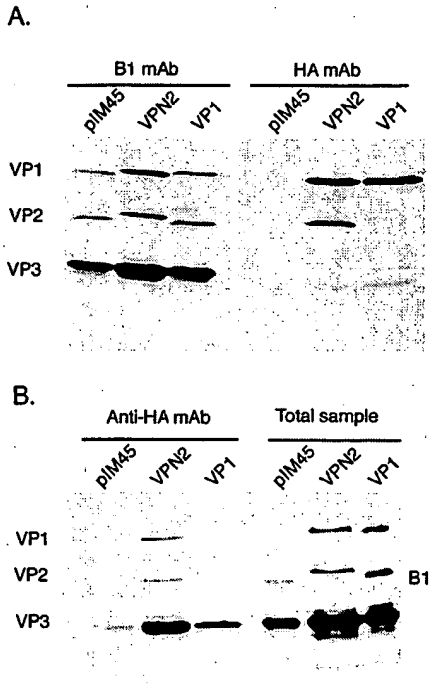

FIG. 6. Immunoprecipitation analysis of VP1 and VPN2 HA insertion mutants to determine the accessibility of the HA epitope. (A) Western blot analysis of iodixanol gradient-purified viruses with either B1 (left) or HA (right) MAb. (B) Iodixanol gradient and heparan column-purified viruses were precipitated with HA antibody coupled to agarose beads. The bound virus (Anti-HA mAb lanes) was eluted with SDS sample buffer and detected by Western blotting using MAb B1. For comparison, virus that had not been treated with HA MAb (Total sample) was also Western blotted with the B1 antibody.

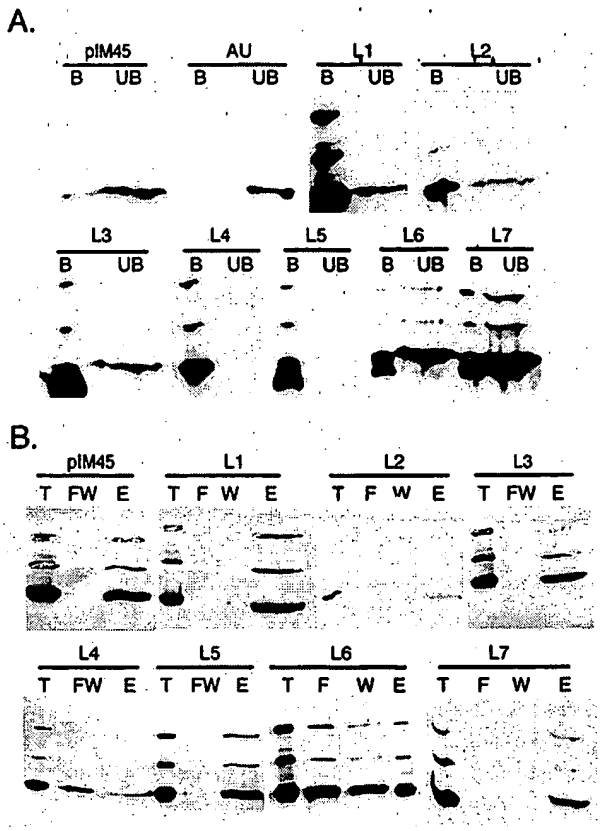

FIG. 7. Properties of HA insertion mutants. (A) Immunoprecipitation of HA loop insertion mutants to determine whether HA is exposed on the capsid surface. Iodixanol gradient and heparan column-purified viruses were incubated with HA MAb beads as described for Fig. 6. The antibody bound (B) and unbound (UB) fractions were separated on SDS–10% gels and detected by Western blotting with MAb B1. As a negative control, AU MAb was used in the panel marked AU. The pIM45 panel contained recombinant virus made with the wt helper plasmid. (B) Heparan binding properties of wt and HA loop insertion mutants. The virus samples were treated as described for Fig. 5. Virus in the starting material (T), flowthrough (F), wash (W), combined flowthrough and wash (FW), or eluate (E) was detected by Western blotting with MAb B1. pIM45 is virus with wt capsid.

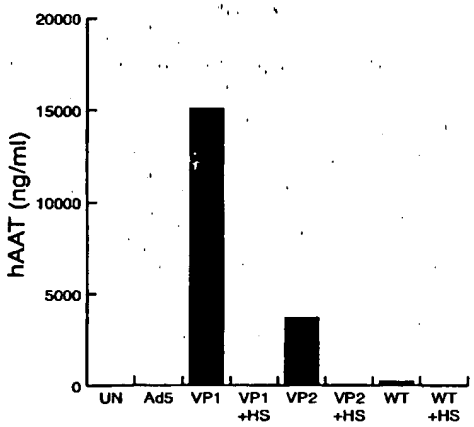

FIG. 8. Infection of IB3 cells with wt and mutant viruses containing a serpin ligand insertion. IB3 cells (1.5×10^5 per 15-mm well) were infected with Ad5 for 60 min at an MOI of 10 and washed twice with medium. The cells then were infected for 60 min at an MOI of 400 with rAAV containing a genome that expressed the hAAT gene under the control of a CMV–β-actin hybrid promoter. Following infection, the cells were washed with medium and incubated at 37°C. At 72 h postinfection, medium samples were taken to determine the AAT concentration by ELISA. All experiments were done in triplicate, and the average for each experiment is shown. WT indicates that rAAV containing a wt AAV capsid (grown by complementation with pIM45) was used. VP1 virus was grown by complementation with a mutant plasmid containing the serpin ligand sequence (FVFLI) substituted for the AAV capsid sequence after aa 34 of the cap ORF. VP2 virus contained a serpin insertion (KFNKPFVFLI) at the N terminus of VP2, aa 138 of the cap ORF. In the +HS samples, rAAV infection was done in the presence of soluble heparan sulfate at a concentration of 2 mg/ml.

entry. When this was done, both wt and mutant infectivity dropped to barely detectable levels (Fig. 8). Taken together, these findings suggested that the serpin-tagged viruses continued to use heparan sulfate proteoglycan as the primary receptor and were using an alternative coreceptor, presumably the serpin receptor.

DISCUSSION

In this study we describe the phenotypes of 93 AAV2 capsid mutants at 59 different positions within the capsid ORF. Several classes of mutants were analyzed, including epitope tag or peptide ligand insertion mutants, alanine scanning mutants, and epitope substitution mutants. From this, we could identify some eight separate phenotypes (Fig. 1; Table 1).

Noninfectious mutants. The bulk of the mutants that were noninfectious either were unable to assemble capsids or the capsids were unstable. These mutants (class 4b) were located predominantly but not exclusively in what are likely to be β-strand structures in the capsid proteins (Fig. 1). Two of these mutants were insertions at the N- and C-terminal residues of VP3, suggesting that both ends of VP3 play a role that is important for capsid assembly or stability. We note that Ruffing et al. (32) have previously characterized deletions of the C terminus of the capsid ORF, and these deletions also were noninfectious.

One noninfectious mutant, *mut*31, produced viable capsids that were empty. This mutant, which consists of a single amino acid substitution (R432A), was apparently defective in packaging viral DNA and is located in putative loop IV (Fig. 1). It is not clear what the mechanism of viral DNA packaging is. Ruffing et al. (33) demonstrated that empty capsids could assemble in the absence of viral DNA. Some studies have suggested that packaging is an active process that requires interaction of Rep proteins with capsid proteins (42) or possibly is coupled with DNA replication (49). Further studies with *mut*31 may be helpful in understanding the mechanism of packaging.

Most of the remaining noninfectious mutants (Fig. 1, class 4a) were capable of assembling capsids and packaging DNA. These are likely to be defective in some aspect of viral entry or uncoating and will require further study to uncover the mechanism of the defect.

Receptor binding mutants. Two of the noninfectious mutants, *mut*40 and L4, were apparently noninfectious because they were unable to bind to heparan sulfate (Fig. 1, class 4d). Heparan sulfate proteoglycan is believed to be the primary cell surface receptor for AAV (37). Three other mutants also were identified as defective for binding heparan sulfate, two partially defective mutants (Fig. 1, class 2c) and one temperature-sensitive mutant (class 3b). Together, the five mutants were distributed into two clusters in loop IV that were separated by 40 aa. The first cluster spanned aa 509 to 520 (*mut*35 and L4); the second was between aa 561 and 591 (*mut*40, *mut*41, and L6). Mutants L4 and L6 consisted of HA epitope insertions into the two heparan binding clusters. These were found to be capable of being immunoprecipitated by HA MAb, confirming that these positions were on the surface of the capsid. We note also that Girod et al. (15) reported that insertion of the L14 epitope at aa 587, the position of our heparan-negative *mut*41 mutant, was capable of targeting the virus to the L14 receptor, thus confirming that this region is on the surface of the capsid. A heparan-negative insertion mutant also was reported by Rabinowitz et al. (30) while this report was in preparation; it fell near the first cluster at aa 522. Taken together, analyses of these mutants suggest that the putative loop IV region contains two blocks of residues that are on the surface of the capsid and involved in heparan sulfate binding.

A heparan binding motif which consists of a negatively charged amino acid cluster of the type XBBBXXBX (where B is a basic amino acid and X is any amino acid) has been identified in several receptors and viruses (19a). Regions containing these clusters also appear to be sensitive to spacing changes. Although no heparan binding consensus motif of this kind was found in our heparan binding mutants, there were basic amino acids near these domains. *mut*35, an insertion at aa 509, was near basic amino acids K507 and H509. Interestingly, K507 is conserved in AAV1, -2, -3, -4, and -6 and in AAV5 is an R. H509 is present only in AAV2 and -3. AAV1, -2, and -3 are known to bind to heparan sulfate, while AAV4 and -5 do not. Additionally, L4, an insertion at aa 520, was near basic amino acids H526 and K527, and L6, an insertion at aa 591, was near R585 and R588. H526 and K527 are conserved except for AAV4 and -5, while R585 and R588 are unique to AAV2. For all of these mutants, the insertions could have disrupted local conformation that hindered normal heparan binding. For *mut*41, R-to-A substitutions at aa 585 and 588 might contribute directly to reduced heparan binding. Finally, *mut*40 did not affect either basic amino acids or spacing within the capsid protein.

Capsid regions that are on the surface of the virus particle. In addition to the heparan binding clusters, several other regions were also present on the capsid surface. These include four of the five putative loop regions (mutants L1 to L7), the N terminus of VP2 (mutant VPN2), and a region within the N terminus of VP1 at amino acid 34 (mutant VP1). HA epitope insertions at these positions were all capable of being immunoprecipitated with anti-HA antibody (Fig. 6 and 7). We note that the L1 insertion mutant at aa 266 had the peculiar phenotype of being partially viable (Table 1) but was not detectable with the A20 MAb, an antibody that recognizes a conformational epitope that is present only in intact viral particles. A

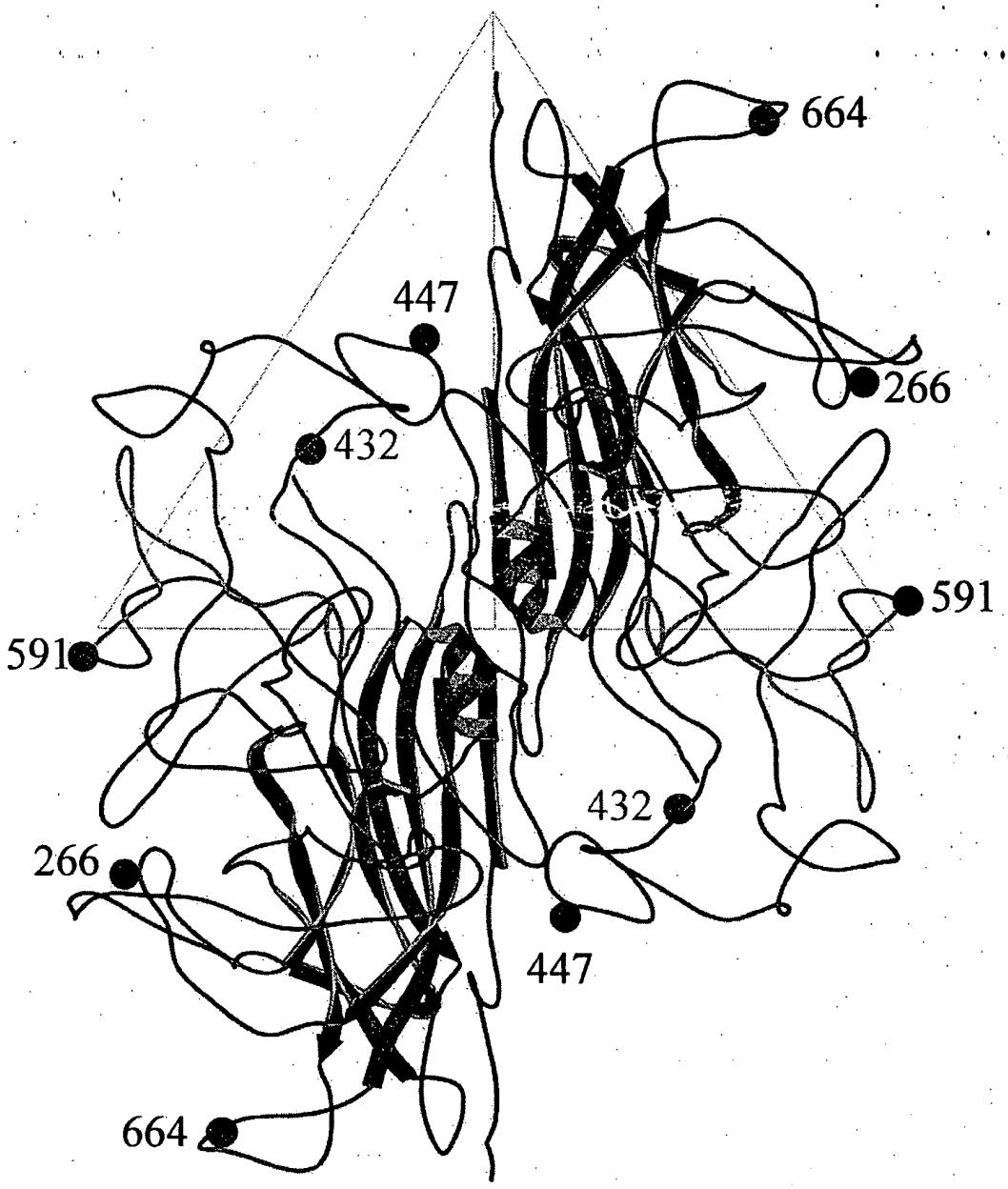

FIG. 9. Ribbon diagrams of a dimer of the AAV VP3 model built based on structural alignments with the VP2 capsid protein of CPV. The view is down an icosahedral twofold axis. The strands of the β-barrel motif are colored blue, and the portion of VP3 in green indicates the heparan binding region. The rest of VP3 is depicted in red. The blue ball identifies the location of residue R432 mutated to an alanine in *mut*31. The gray balls identify the location of residues 266, 477, 591, and 664 (which had HA insertions in mutants L1, L3, L6, and L7, respectively). The large triangle indicates an icosahedral asymmetric unit.

nearby capsid-forming mutant made by Girod et al. (15) at aa 261 was also negative for A20 antibody binding. This suggests that at least part of the epitope for the A20 MAb consists of amino acids between 261 and 266 and confirms that this region is on the surface of the intact particle.

Of the positions identified as being on the surface of the capsid, we found six that potentially are capable of accepting foreign epitope or ligand insertions for retargeting the viral capsid to alternative receptors. These are the N-terminal region of VP1 (near aa 34), the N terminus of VP2 (aa 138), the loop I region (aa 266), the loop IV region (near aa 447 and 591), and the loop V region (aa 664). All of these locations were capable of tolerating an HA (or serpin) insertion and produced recombinant virus titers that were within 1 to 2 logs of the wt value. Furthermore, HA epitope insertions at these positions were capable of being immunoprecipitated with anti-HA antibody (Fig. 6 and 7). Two of these positions, when tested with a serpin ligand insertion or substitution, produced virus that was much more infectious on IB3 cells than wt virus. Curiously, both serpin mutants were still inhibited by soluble heparan sulfate, suggesting that heparan sulfate proteoglycan was still the primary receptor for these mutants and that the serpin receptor was being used as an alternative coreceptor. It is conceivable that one or both of these capsid positions is

involved in binding to one or both of the proteins that normally act as coreceptors for wt virus, fibroblast growth factor (28), or integrin $\alpha_v\beta_5$ (36). This would explain their partial defect on 293 cells and the recovery of infectivity on IB3 cells. Further studies will be needed to test this possibility.

Mutants with unstable capsids and temperature-sensitive phenotypes. Three mutants, *mut*21, *mut*27, and *mut*39, were found to have capsids that were unstable when purified through an iodixanol gradient. Iodixanol is an iso-osmotic gradient purification method that appears to be gentler than CsCl centrifugation (51). Thus, these mutants appear to be particularly sensitive to capsid denaturation. *mut*21 and *mut*27 are in putative β sheets, and *mut*39 is in loop IV. It is worth noting that Rabinowitz et al. (30) also isolated an unstable capsid mutant at aa 247 that is near the *mut*21 position, aa 254. *mut*27 is also one of five temperature-sensitive mutants isolated during this study. The temperature-sensitive mutants and the unstable capsid mutants should prove useful in future studies for identifying steps in the capsid assembly or the infection process.

Viable and partially defective mutants. The two largest classes of mutants isolated were either wt (class 1) or partially defective (class 2a) with no identifiable defect (Fig. 1). Both class 1 and class 2a mutants were distributed either in the VP1 and VP2 unique regions or in the predicted loop regions of the capsid protein. We naively assumed that class 1 mutant positions, which produced viable capsids after substitution of two to five alanine residues, were regions that were nonessential for capsid assembly or stability and therefore should accommodate other kinds of substitutions. However, when serpin or FLAG epitopes were substituted at many of these sites, most of the mutants were nonviable, with the exception of aa 34 in VP1. Indeed, many of these viruses were negative for capsid assembly and should also be useful for identifying possible intermediates in capsid assembly.

Ruffing et al. (33) showed previously that VP1 and VP2 but not VP3 contained nuclear localization signals (NLS), and three putative NLS are located in the VP1/VP2 region at aa 121 to 125, 141 to 145, and 167 to 171. Hoque et al. (19b) have shown that aa 167 to 172 were sufficient to target VP2 to the nucleus, although their experiments did not rule out possible redundancy with the other two putative NLS sequences. All three of these putative signals were targeted with alanine scanning mutants (*mut*12, *mut*13, and *mut*15) in our study. Two of these mutants, *mut*12 and *mut*15, were partially defective, and the inactivation of an NLS may be the reason for their phenotype (19b, 33). We note that *mut*15 should have eliminated the NLS identified by Hoque and colleagues. The fact that *mut*15 was only partially defective suggests that there may be an alternative, redundant NLS sequences that are used by the capsid proteins. The third mutant (*mut*13) was classified as viable, but it also showed a lower than wt titer (Fig. 1).

Molecular computer graphics construction of an AAV model and structural localization of mutant residues. Because the AAV crystal structure is not available, the atomic coordinates of CPV VP2 (PDB accession no. 4DPV) were interactively mutated using the program O (20) to generate a homology-based model of the AAV capsid, using modifications of the alignments of the AAV major capsid protein (VP3) with the VP2 capsid protein of CPV (9, 15). The mutations were followed by refinement constrained with standard geometry in the O database. The model provided a means for preliminary structural identification of the heparan receptor attachment sites in the surface depression (dimple) near the twofold icosahedral axes of the capsid, surface loop regions which can tolerate foreign peptide sequence insertions, and a possible explanation for the phenotype of *mut*31 (Fig. 9).

The topographic location of the putative heparan binding region is consistent with regions that have been suggested as being involved in host cellular factor(s) recognition and implicated in tissue tropism and *in vivo* pathogenicity for other parvoviruses (3, 4, 24, 39). It is of interest that the putative heparan binding site is adjacent to a region of the AAV capsid that contains a peptide insert when the AAV VP3 sequence is compared to that of CPV VP2 and the VP2 of most of the other autonomous parvovirus sequences (9). Also a similar insertion of peptide sequences compared to CPV (although not in a homologous region of the VP2 to that observed in AAV) is present in the capsid of Aleutian mink disease parvovirus and minute virus of mice, proximal to residues in the dimple depression which are implicated in tissue tropism (24). Thus, these insertions may be capsid surface adaptations that enable the capsids to recognize different receptors during infection. In the case of AAV, its dimple peptide insertion, which is absent in the other parvoviruses, may enable it to recognize heparan sulfate, which has not been implicated in cellular infectivity by any other parvovirus.

The model also clearly shows that regions of the capsid which tolerated the insertions of the HA epitope (i.e., at residues 266, 447, 591, and 664) are on the surface loops present between the β strands of the β-barrel motif (Fig. 9). The β-barrel motif forms the core contiguous shell of parvovirus capsids, while the surface loops make up the surface decorations, dictating the strain-specific biological properties of the members. The observation that these surface regions can tolerate foreign peptide insertion is an indication that they are not involved in the interactions that govern capsid assembly.

Finally, the model provides a possible explanation for the observation that *mut*31 (R432A) is able to form only empty particles. In the unassembled VP3 monomer, the side chain of R432, points toward the interior of the capsid and would most likely be in contact with DNA. If recognition and encapsidation of AAV DNA precede final capsid assembly and involve oligomeric intermediates, then R432 contacts with DNA may be essential for initiating capsid assembly around a nascent DNA strand.

In summary, we have reported a preliminary analysis of mutants at 59 positions within the AAV2 capsid ORF. We have identified regions in the capsid proteins that affect infectivity, capsid formation, capsid stability, DNA packaging, and receptor binding. These mutants should be valuable for defining the functional domains of AAV capsid proteins and for dissecting the molecular mechanism of viral entry. Additionally, we have defined a number of regions in the capsid gene at which foreign ligands can be inserted and have demonstrated that insertion of a foreign receptor ligand at some of these positions can change the tropism of the virus. This is the first step in the development of the next generation of AAV vectors, which can be targeted to specific cellular receptors or tissues.

ACKNOWLEDGMENTS

We thank J. Kleinschmidt for kindly providing MAbs A20 and B1. We also thank R. J. Samulski for providing plasmid pXX6. We acknowledge the Vector Core Laboratory at the Powell Gene Therapy Center, University of Florida Medical School, for technical assistance on rAAV production. We thank Corrine Abernathy, Daniel Lackner, and Eric Kolbrener for help on this project.

This work was supported by grants PO1 HL59412, PO1 HL51811, and PO1 NS36302 from the National Institutes of Health.

REFERENCES

1. **Agbandje, M., S. Kajigaya, R. McKenna, N. S. Young, and M. G. Rossmann.** 1994. The structure of human parvovirus B19 at 8 Å resolution. Virology **203:** 106–115.

2. **Agbandje, M., R. McKenna, M. G. Rossmann, M. L. Strassheim, and C. R. Parrish.** 1993. Structure determination of feline panleukopenia virus empty particles. Proteins **16**:155–171.
3. **Agbandje-McKenna, M., A. L. Llamás-Saiz, F. Wang, P. Tattersall, and M. G. Rossmann.** 1998. Functional implications of the structure of the murine parvovirus, minute virus of mice. Structure **6**:1369–1381.
4. **Barbis, D. P., S. F. Chang, and C. R. Parrish.** 1992. Mutations adjacent to the dimple of the canine parvovirus capsid structure affect sialic acid binding. Virology **191**:301–308.
5. **Berns, K. I., and R. A. Bohenzky.** 1987. Adeno-associated viruses: an update. Adv. Virus Res. **32**:243–306.
6. **Berns, K. I., and C. Giraud.** 1995. Adenovirus and adeno-associated virus as vectors for gene therapy. Ann. N. Y. Acad. Sci. **772**:95–104.
7. **Buller, R. M., J. E. Janik, E. D. Sebring, and J. A. Rose.** 1981. Herpes simplex virus types 1 and 2 completely help adenovirus-associated virus replication. J. Virol. **40**:241–247.
8. **Casto, B. C., J. A. Armstrong, R. W. Atchison, and W. M. Hammon.** 1967. Studies on the relationship between adeno-associated virus type 1 (AAV-1) and adenoviruses. II. Inhibition of adenovirus plaques by AAV; its nature and specificity. Virology **33**:452–458.
9. **Chapman, M. S., and M. G. Rossmann.** 1993. Structure, sequence, and function correlations among parvoviruses. Virology **194**:491–508.
10. **Chiorini, J. A., L. Yang, Y. Liu, B. Safer, and R. M. Kotin.** 1997. Cloning of adeno-associated virus type 4 (AAV4) and generation of recombinant AAV4 particles. J. Virol. **71**:6823–6833.
11. **Cunningham, B. C., and J. A. Wells.** 1989. High resolution epitope mapping of hGH-receptor interactions by alanine-scanning mutagenesis. Science **244**: 1081–1085.
12. **Fisher, K. J., G. P. Gao, M. D. Weitzman, R. DeMatteo, J. F. Burda, and J. M. Wilson.** 1996. Transduction with recombinant adeno-associated virus for gene therapy is limited by leading-strand synthesis. J. Virol. **70**:520–532.
13. **Fisher-Adams, G., K. K. Wong, Jr., G. Podsakoff, S. J. Forman, and S. Chatterjee.** 1996. Integration of adeno-associated virus vectors in CD34+ human hematopoietic progenitor cells after transduction. Blood **88**:492–504.
14. **Flotte, T. R., S. A. Afione, C. Conrad, S. A. McGrath, R. Solow, H. Oka, P. L. Zeitlin, W. B. Guggino, and B. J. Carter.** 1993. Stable in vivo expression of the cystic fibrosis transmembrane conductance regulator with an adeno-associated virus vector. Proc. Natl. Acad. Sci. USA **90**:10613–10617.
15. **Girod, A., M. Ried, C. Wobus, H. Lahm, K. Leike, J. Kleinschmidt, G. Deleage, and M. Hallek.** 1999. Genetic capsid modifications allow efficient re-targeting of adeno-associated virus type 2. Nat. Med. **5**:1438.
16. **Gnatenko, D., T. E. Arnold, S. Zolotukhin, G. J. Nuovo, N. Muzyczka, and W. F. Bahou.** 1997. Characterization of recombinant adeno-associated virus-2 as a vehicle for gene delivery and expression into vascular cells. J. Investig. Med. **45**:87–98.
17. **Graham, F. L., J. Smiley, W. C. Russell, and R. Nairn.** 1977. Characteristics of a human cell line transformed by DNA from human adenovirus type 5. J. Gen. Virol. **36**:59–74.
18. **Grimm, D., A. Kern, M. Pawlita, F. Ferrari, R. Samulski, and J. Kleinschmidt.** 1999. Titration of AAV-2 particles via a novel capsid ELISA: packaging of genomes can limit production of recombinant AAV-2. Gene Ther. **6**:1322–1330.
19. **Hermonat, P. L., M. A. Labow, R. Wright, K. I. Berns, and N. Muzyczka.** 1984. Genetics of adeno-associated virus: isolation and preliminary characterization of adeno-associated virus type 2 mutants. J. Virol. **51**:329–339.

19a. **Hileman, R. E., J. R. Fromm, J. M. Weiler, and R. J. Linhardt.** 1998. Glycosaminoglycan-protein interactions: definition of consensus sites in glycosaminoglycan binding proteins. Bioessays **2**:156–167.

19b. **Hoque, M., K. Ishizu, A. Matsumoto, S. I. Han, F. Arisaka, M. Takayama, K. Suzuki, K. Kato, T. Kanda, H. Watanabe, and H. Handa.** 1999. Nuclear transport of the major capsid protein is essential for adeno-associated virus capsid formation. J. Virol. **73**:7912–7915.

20. **Jones, T. A., J. Y. Zou, S. W. Cowan, and Kjeldgaard.** 1991. Improved methods for binding protein models in electron density maps and the location of errors in these models. Acta Crystallogr. A **47**:110–119.
21. **Kaplitt, M. G., P. Leone, R. J. Samulski, X. Xiao, D. W. Pfaff, K. L. O'Malley, and M. J. During.** 1994. Long-term gene expression and phenotypic correction using adeno-associated virus vectors in the mammalian brain. Nat. Genet. **8**:148–154.
22. **Klein, R. L., E. M. Meyer, A. L. Peel, S. Zolotukhin, C. Meyers, N. Muzyczka, and M. A. King.** 1998. Neuron-specific transduction in the rat septohippocampal or nigrostriatal pathway by recombinant adeno-associated virus vectors. Exp. Neurol. **150**(2):183–194.
23. **McCarty, D. M., M. Christensen, and N. Muzyczka.** 1991. Sequences required for coordinate induction of adeno-associated virus p19 and p40 promoters by Rep protein. J. Virol. **65**:2936–2945.
24. **McKenna, R., N. H. Olson, P. R. Chipman, T. S. Baker, T. F. Booth, J. Christensen, B. Aasted, J. M. Fox, M. E. Bloom, J. B. Wolfinbarger, and M. Agbandje-McKenna.** 1999. Three-dimensional structure of Aleutian mink disease parvovirus: implications for disease pathogenicity. J. Virol. **73**:6882–6891.
25. **Muralidhar, S., S. P. Becerra, and J. A. Rose.** 1994. Site-directed mutagenesis of adeno-associated virus type 2 structural protein initiation codons: effects on regulation of synthesis and biological activity. J. Virol. **68**:170–176.
26. **Muzyczka, N.** 1992. Use of adeno-associated virus as a general transduction vector for mammalian cells. Curr. Top. Microbiol. Immunol. **158**:97–129.
27. **Ponnazhagan, S., P. Mukherjee, X. S. Wang, K. Qing, D. M. Kube, C. Mah, C. Kurpad, M. C. Yoder, E. F. Srour, and A. Srivastava.** 1997. Adeno-associated virus type 2-mediated transduction in primary human bone marrow-derived CD34$^+$ hematopoietic progenitor cells: donor variation and correlation of transgene expression with cellular differentiation. J. Virol. **71**:8262–8267.
28. **Qing, K., C. Mah, J. Hansen, S. Zhou, V. Dwarki, and A. Srivastava.** 1999. Human fibroblast growth factor receptor 1 is a co-receptor for infection by adeno-associated virus 2. Nat. Med. **5**:71–77.
29. **Rabinowitz, J. E., and J. Samulski.** 1998. Adeno-associated virus expression systems for gene transfer. Curr. Opin. Biotechnol. **9**:470–475.
30. **Rabinowitz, J. E., W. Xiao, and R. J. Samulski.** 1999. Insertional mutagenesis of AAV2 capsid and the production of recombinant virus. Virology **265**: 274–285.
31. **Rossmann, M. G.** 1989. The canyon hypothesis. Hiding the host cell receptor attachment site on a viral surface from immune surveillance. J. Biol. Chem. **264**:14587–14590.
32. **Ruffing, M., H. Heid, and J. A. Kleinschmidt.** 1994. Mutations in the carboxy terminus of adeno-associated virus 2 capsid proteins affect viral infectivity: lack of an RGD integrin-binding motif. J. Gen. Virol. **75**:3385–3392.
33. **Ruffing, M., H. Zentgraf, and J. A. Kleinschmidt.** 1992. Assembly of viruslike particles by recombinant structural proteins of adeno-associated virus type 2 in insect cells. J. Virol. **66**:6922–6930.
34. **Song, S., M. Morgan, T. Ellis, A. Poirier, K. Chesnut, J. Wang, M. Brantly, N. Muzyczka, B. J. Byrne, M. Atkinson, and T. R. Flotte.** 1998. Sustained secretion of human alpha-1-antitrypsin from murine muscle transduced with adeno-associated virus vectors. Proc. Natl. Acad. Sci. USA **95**:14384–14388.
35. **Srivastava, A., E. W. Lusby, and K. I. Berns.** 1983. Nucleotide sequence and organization of the adeno-associated virus 2 genome. J. Virol. **45**:555–564.
36. **Summerford, C., J. S. Bartlett, and R. J. Samulski.** 1999. AlphaVbeta5 integrin: a co-receptor for adeno-associated virus type 2 infection. Nat. Med. **5**:78–82.
37. **Summerford, C., and R. J. Samulski.** 1998. Membrane-associated heparan sulfate proteoglycan is a receptor for adeno-associated virus type 2 virions. J. Virol. **72**:1438–1445.
38. **Tratschin, J. D., I. L. Miller, and B. J. Carter.** 1984. Genetic analysis of adeno-associated virus: properties of deletion mutants constructed in vitro and evidence for an adeno-associated virus replication function. J. Virol. **51**:611–619.
39. **Tresnan, D. B., L. Southard, W. Weichert, J. Y. Sgro, and C. R. Parrish.** 1995. Analysis of the cell and erythrocyte binding activities of the dimple and canyon regions of the canine parvovirus capsid. Virology **211**:123–132.
40. **Tsao, J., M. S. Chapman, M. Agbandje, W. Keller, K. Smith, H. Wu, M. Luo, T. J. Smith, M. G. Rossmann, R. W. Compans, et al.** 1991. The three-dimensional structure of canine parvovirus and its functional implications. Science **251**:1456–1464.
41. **Tsao, J., M. S. Chapman, H. Wu, M. Agbandje, W. Keller, and M. G. Rossmann.** 1992. Structure determination of monoclinic canine parvovirus. Acta Crystallogr. B **48**:75–88.
42. **Weger, S., M. Wendland, J. A. Kleinschmidt, and R. Heilbronn.** 1999. The adeno-associated virus type 2 regulatory proteins Rep78 and Rep68 interact with the transcriptional coactivator PC4. J. Virol. **73**:260–269.
43. **Wistuba, A., A. Kern, S. Weger, D. Grimm, and J. A. Kleinschmidt.** 1997. Subcellular compartmentalization of adeno-associated virus type 2 assembly. J. Virol. **71**:1341–1352.
44. **Wistuba, A., S. Weger, A. Kern, and J. A. Kleinschmidt.** 1995. Intermediates of adeno-associated virus type 2 assembly: identification of soluble complexes containing Rep and Cap proteins. J. Virol. **69**:5311–5319.
45. **Xiao, X., J. Li, and R. J. Samulski.** 1996. Efficient long-term gene transfer into muscle tissue of immunocompetent mice by adeno-associated virus vector. J. Virol. **70**:8098–8108.
46. **Xiao, X., J. Li, and R. J. Samulski.** 1998. Production of high-titer recombinant adeno-associated virus vectors in the absence of helper adenovirus. J. Virol. **72**:2224–2232.
47. **Yang, Q., M. Mamounas, G. Yu, S. Kennedy, B. Leaker, J. Merson, F. Wong-Staal, M. Yu, and J. R. Barber.** 1998. Development of novel cell surface CD34-targeted recombinant adeno-associated virus vectors for gene therapy. Hum. Gene Ther. **9**:1929–1937.
48. **Zhou, S. Z., S. Cooper, L. Y. Kang, L. Ruggieri, S. Heimfeld, A. Srivastava, and H. E. Broxmeyer.** 1994. Adeno-associated virus 2-mediated high efficiency gene transfer into immature and mature subsets of hematopoietic progenitor cells in human umbilical cord blood. J. Exp. Med. **179**:1867–1875.
49. **Zhou, X., and N. Muzyczka.** 1998. In vitro packaging of adeno-associated virus DNA. J. Virol. **72**:3241–3247.
50. **Ziady, A. G., J. C. Perales, T. Ferkol, T. Gerken, H. Beegen, D. H. Perlmutter, and P. B. Davis.** 1997. Gene transfer into hepatoma cell lines via the serpin enzyme complex receptor. Am. J. Physiol. **273**(2 Pt. 1):G545–G552.
51. **Zolotukhin, S., B. J. Byrne, E. Mason, I. Zolotukhin, M. Potter, K. Chesnut, C. Summerford, R. J. Samulski, and N. Muzyczka.** 1999. Recombinant adeno-associated virus purification using novel methods improves infectious titer and yield. Gene Ther. **6**:973–985.

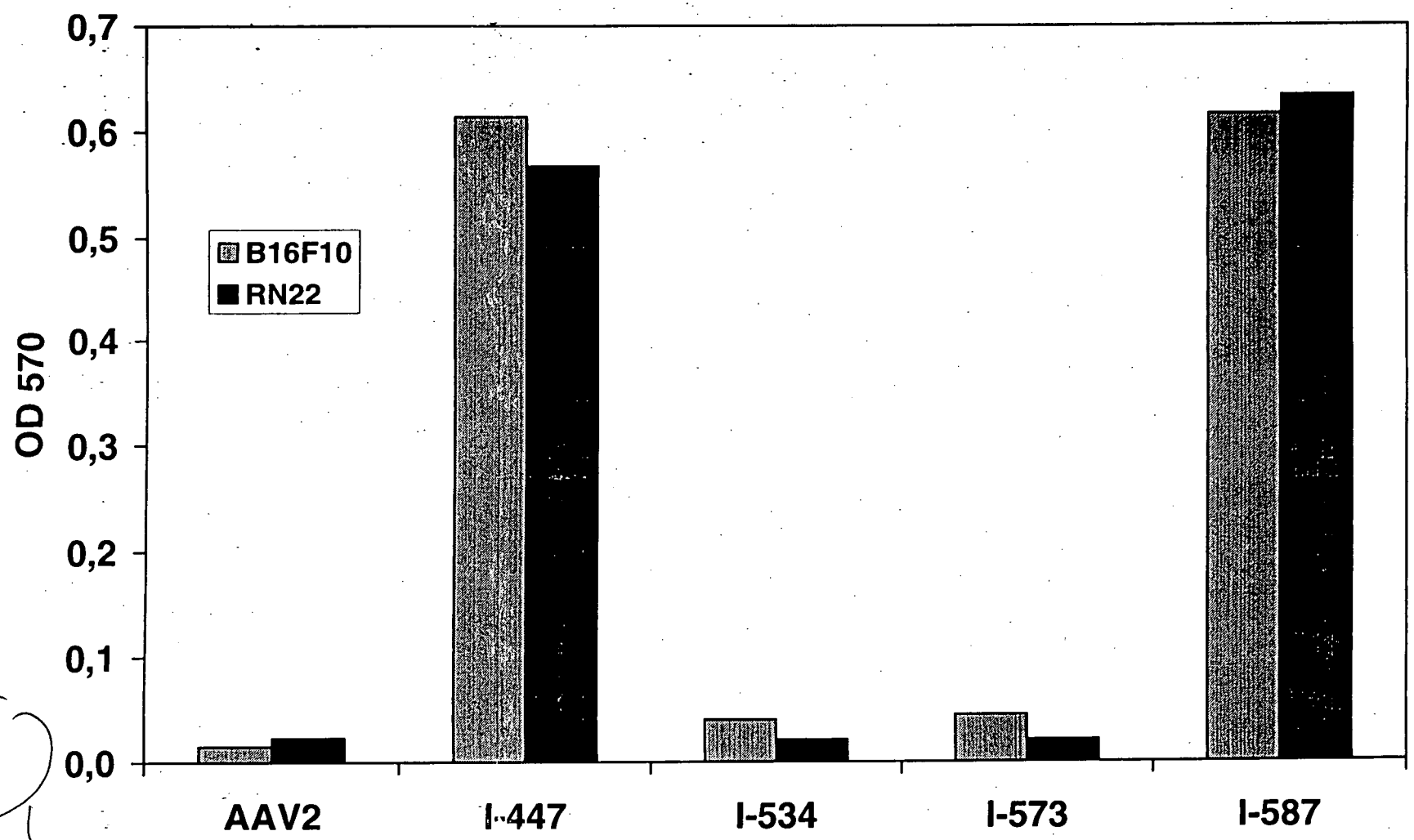

Fig. 2

FIGURE 2

Fig. 1

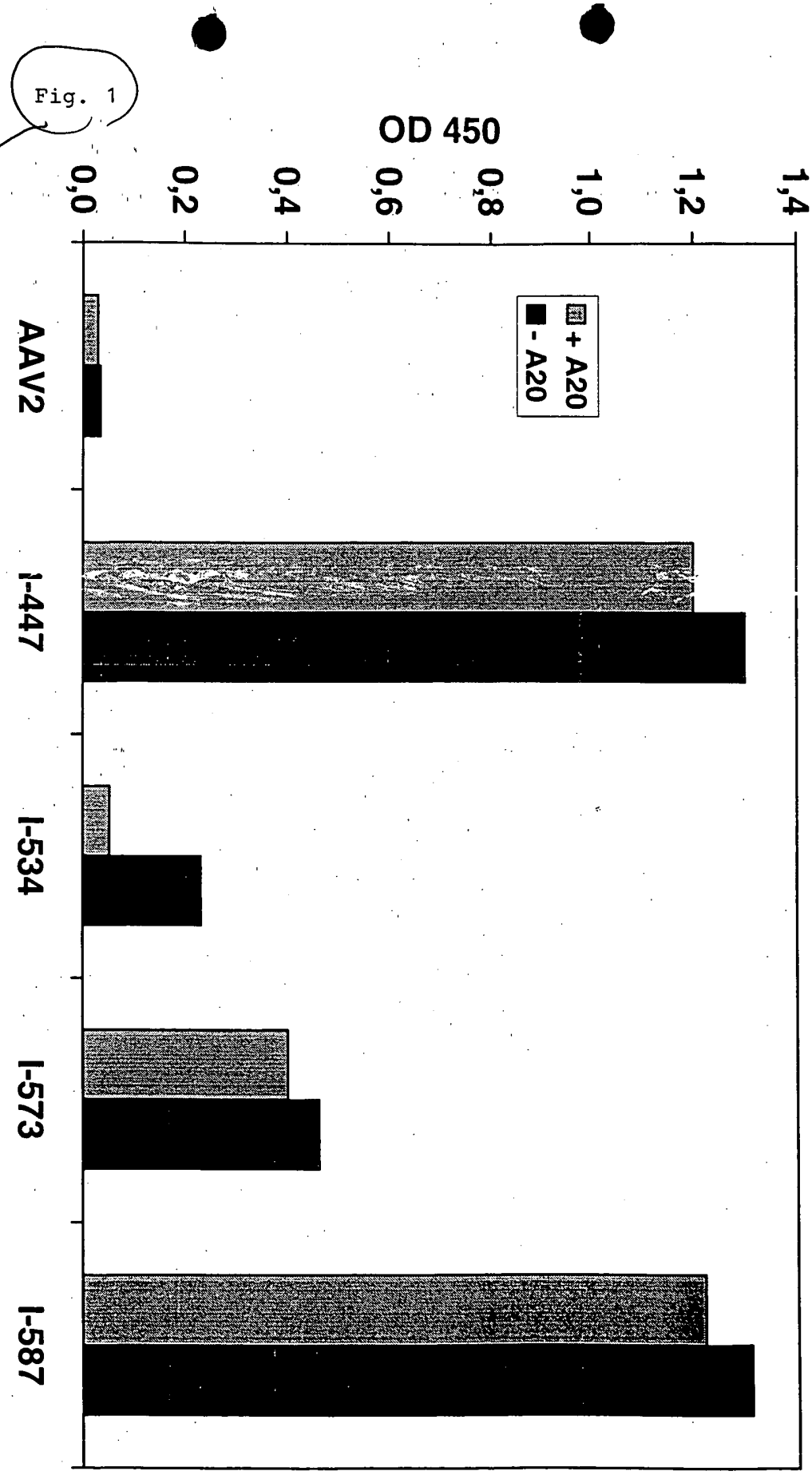

FIGURE 1

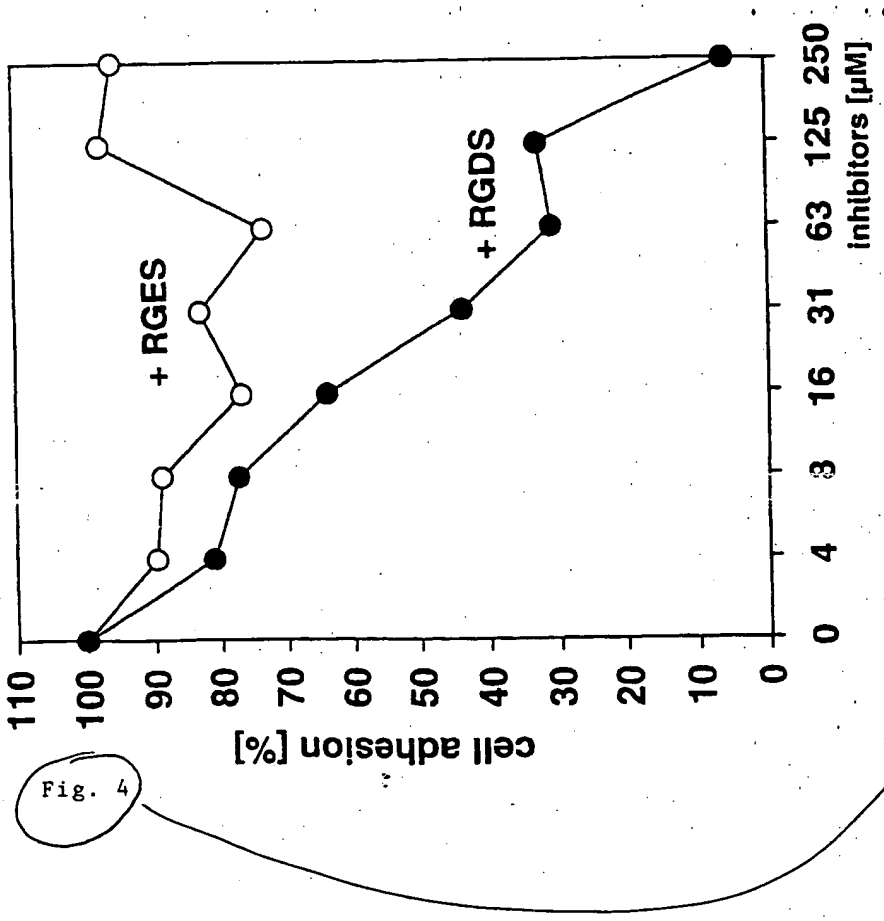

Fig. 4

FIGURE 4

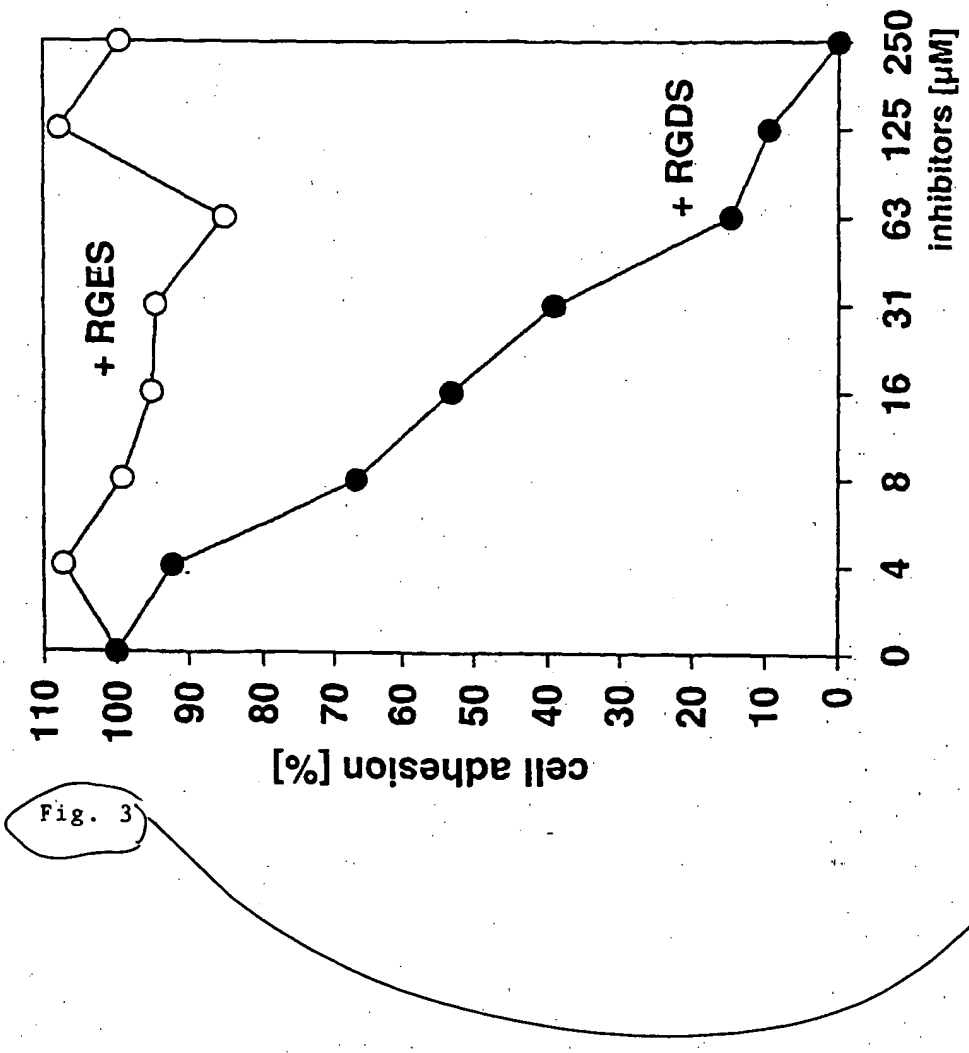

Fig. 3

FIGURE 3